Eur J Forest Res (2010) 129:749–770
DOI 10.1007/s10342-010-0381-4

REVIEW

Retrieval of forest structural parameters using LiDAR remote sensing

Martin van Leeuwen · Maarten Nieuwenhuis

Received: 14 June 2009 / Revised: 1 March 2010 / Accepted: 15 March 2010 / Published online: 1 May 2010

Abstract In this paper, a literature overview is presented on the use of laser rangefinder techniques for the retrieval of forest inventory parameters and structural characteristics. The existing techniques are ordered with respect to their scale of application (i.e. spaceborne, airborne, and terrestrial laser scanning) and a discussion is provided on the efficiency, precision, and accuracy with which the retrieval of structural parameters at the respective scales has been attained. The paper further elaborates on the potential of LiDAR (Light Detection and Ranging) data to be fused with other types of remote sensing data and it concludes with recommendations for future research and potential gains in the application of LiDAR for the characterization of forests.

Keywords LiDAR · Forest inventory · Remote sensing

Introduction

Remote sensing has been used successfully to retrieve forest structural parameters (Roberts et al. 2007) that can be used to support decision-making at the forest management level (Reese et al. 2002). These remote sensing techniques rely on statistical or physical relationships between electromagnetic scattering characteristics of the vegetated Earth surface, and parameters of interest to management, such as biodiversity, biomass, net and gross primary production (NPP/GPP), leaf and basal area or simply tree height (e.g. Drake et al. 2002; Gitelson 2004; Koetz et al. 2007; Smith et al. 2008; Turner et al. 2003).

Since many minerals, as well as water and pigments such as chlorophyll, exhibit strong absorption peaks in the visible and infrared spectrum, optical remote sensing techniques are highly suited for a wide range of analyses (Kumar et al. 2002; Lillesand et al. 2004). Microwave remote sensing, on the other hand, has the capacity to penetrate forest canopies deeply owing to its larger wavelengths and remains a highly applicable tool for the detection of structural complexity and variation in forest canopies.

A recent sensor technology is LiDAR (Light Detection and Ranging) and currently attracts much attention from the forestry community as a rapid and efficient tool for forest inventories. LiDAR is similar to radar in that it exploits electromagnetism for the detection and ranging of spatial objects, and it is similar to optical forms of remote sensing in the sense that it uses optics for the refraction of these electromagnetic waves. While LiDAR is subjected to the same scattering characteristics of light as conventional optical remote sensing techniques, the technology allows ranging of objects and this is achieved by measuring the time of flight between emitted pulses and their received reflections. In combination with accurate position and attitude sensors, LiDAR allows the remote measure of forest structure from airborne or spaceborne platforms.

To aid potential users in their preparations to make use of this emerging technique, this paper provides an overview of the use of LiDAR remote sensing in forestry

Communicated by J. Müller.

M. van Leeuwen (✉)
Department of Forest Resources Management,
University of British Columbia, 2424 Main Mall,
Vancouver, BC V6T 1Z4, Canada
e-mail: mvanleeu@interchange.ubc.ca

M. van Leeuwen · M. Nieuwenhuis
UCD Forestry, Agriculture and Food Science Centre,
University College Dublin, Belfield, Dublin 4, Ireland

applications and presents the different LiDAR techniques that are available and complements the information on LiDAR remote sensing presented in previous review papers such as by Lim et al. (2003) and Roberts et al. (2007).

In this paper, algorithms for retrieving forest structural parameters from LiDAR data are mentioned and the relative advantages of individual LiDAR techniques are evaluated against each other, as well as against conventional techniques of remote sensing. Finally, the potential to fuse LiDAR with other remote sensing techniques to improve the retrieval of forest biophysical parameters is discussed.

LiDAR functionality

The use of LiDAR for forest inventory purposes has been reported as early as the beginning of the 1980s (Lim et al. 2003), but before that, LiDAR remote sensing had already been used for the creation of digital elevation models (DEMs) and the retrieval of atmospheric particle concentrations (Ritchie 1996). According to Flamant (2005), the name LiDAR has been coined in 1953 by Middleton and Spilhaus (1953), based on its analogy with radar. LiDAR uses a highly collimated beam of laser light, although non-laser light sources may be used as well (Wehr and Lohr 1999). The highly collimated beam gives the advantage of having an energy-efficient means of ranging relatively small objects and discerning a finer spatial detail than radar allows for. Ranging of hit objects is achieved by measuring the time of flight between the transmitted and received energy. Using moving platforms, retrieval of target objects in a three-dimensional space is attained by accurate calculation of the position and attitude of the sensor platform through the use of global positioning systems (GPS) coupled with inertial navigation systems (INS) that measure 3D rotational rate and acceleration of the moving platform. Using ground-based or terrestrial LiDAR, such inertial systems are not needed and the retrieved data may be referenced in a local coordinate frame. The size of the laser beam is either indicated by its beam divergence, typically in mrad (milli radians = 1/1,000 of a radian) or by its footprint that specifies the cross-sectional diameter of the beam at the reflecting surface and at a specified distance (Goodwin et al. 2006). LiDAR scanners may allow recording of single echoes from laser shots, or multiple returns from a number of objects located within the laser footprint in the case of discrete return LiDAR, or as a continuous distribution of returned energy, in the case of waveform LiDAR. LiDAR scanning is achieved by either rotating and/or oscillating mirrors or by a series of fibre optics directing the laser beam to its target location (Wehr and Lohr 1999). The common wavelength used in LiDAR remote sensing for forest inventory practices is 1.064 μm

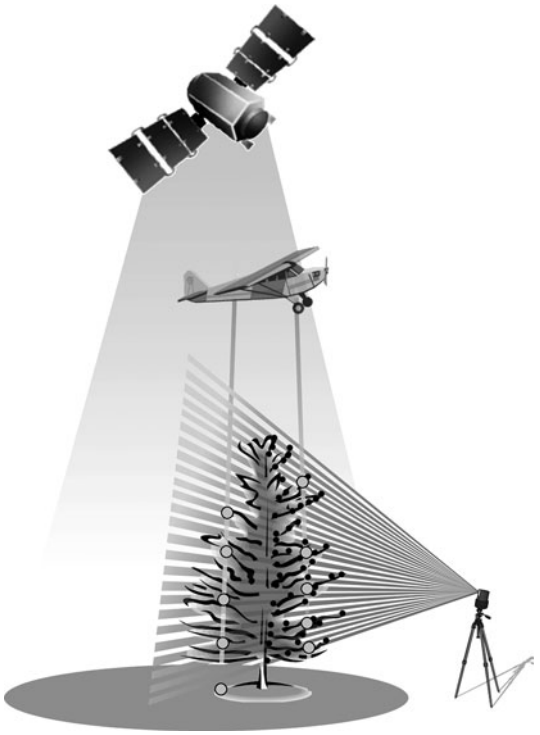

Fig. 1 Spaceborne, airborne, and terrestrial LiDAR remote sensing and their inherent scales of operation

(Wehr and Lohr 1999) and has been chosen for its penetrative capacity through the atmosphere and typical reflectance characteristics of vegetation reaching a maximum in the near-infrared (Kumar et al. 2002).

The different platform types that laser scanning operate from (i.e. ground-based, airborne, spaceborne) allow for a variety of information to be acquired with relative ease, whether large scale, small scale, stand level, or at the level of the individual trees, with each platform type suited to specific forest inventory information needs (Fig. 1).

Airborne LiDAR

A variety of airborne LiDAR sensors are available today. For forest inventory purposes, most use is made of discrete return LiDAR scanners. Popular scanners are those from the Optech ALTM-series, Leica ALS-series, RIEGL LMS-series, and the TopoSys Falcon series. Airborne LiDAR scanners typically are able to register first/last, or multiple returns. Since LiDAR and camera data can be georeferenced based on the same direct exterior orientation (direct EO) techniques, LiDAR scanners can easily be equipped with an additional camera system that can aid in the interpretation of LiDAR returns. Full-waveform airborne LiDAR systems are also available, although their use for forestry applications is concentrated in the scientific

domain. Two examples of full waveform scanners are SLICER and LVIS, both developed by NASA, the specifications of which have been documented in Blair et al. (1999) and Koetz et al. (2007). Recently, commercial full-waveform scanners have become available through, e.g. the RIEGL LMS-Q560, Optech ALTM 3100, TopEye MK II (Hug et al. 2004; Wagner et al. 2006; Kirchhof et al. 2008). Due to cost-efficiency and scale of operation, airborne LiDAR has received by far the most attention for large area retrieval of forest structural parameters.

Tree height

Most attention in retrieving structural parameters from LiDAR data has been paid to the retrieval of tree height, and plot height averages such as Lorey's mean height, predominant tree height, and average tree height, but the technique also allows for individual tree measurements after segmentation of the LiDAR point cloud. Various segmentation approaches have been proposed in a number of studies with varying degrees of success (Heurich 2008; Chen et al. 2006; Popescu and Wynne 2004; Rahman and Gorte 2009). Validation of field and remotely sensed tree height is sometimes difficult due to differences in scale of the field observations and LiDAR acquisitions (Zhao et al. 2009), and challenges to collocate the two (Popescu et al. 2002). These aspects of scale need to be taken into consideration when the suitability of LiDAR remote sensing for forest inventory is assessed and comparisons with other sources of information are made. Furthermore, differences in definition of height measures complicate the task of comparing LiDAR-derived height metrics among different studies (Lovell et al. 2005). For example, mean tree height may be taken as the average height of dominant and co-dominant trees (Lefsky et al. 2007), whereas others may attempt to include the contribution of suppressed trees (Lee and Lucas 2007; Maltamo et al. 2004).

Plot level tree height estimates

Næsset and Økland (2002) retrieved average stand height (Lorey's mean height) accurately with a standard deviation of 1.49 m (7.6% of plot mean height), yielding an R^2 of 0.91. The plots, located in southeast Norway, were dominated by Norway spruce (*Picea abies* L. Karst). The regression equations used to estimate the tree heights were obtained through multiple regression analysis on the natural logarithm of maximum return height of last returns. In a follow-up study, Næsset et al. (2005) assessed the accuracy of several regression techniques (Ordinary Least Squares, Seemingly Unrelated Regression, and Partial Least Squares) to retrieve plot height and other structural parameters. The study showed no increase in accuracy of parameter retrieval when the more complex statistical techniques were used; therefore, the authors recommended the use of ordinary least squares regression for height retrieval. Andersen et al. (2005) derived structural information from LiDAR data in the Pacific Northwest, using linear regression equations of quantile heights, maximum and mean LiDAR heights, coefficient of variation (CV) defined as the standard deviation divided by the mean, and the fraction of retrieved LiDAR returns from the canopy. The study was conducted in western Washington State, USA. Canopy height was accurately determined based on quantile heights and the fraction of retrieved LiDAR returns from the canopy. A strong relationship between LiDAR-derived metrics and field measured plot-level canopy height was found, which explained 98% of variation, with a RMSE of 1.5 m. This RMSE value was obtained from a leave-one-out cross validation procedure. Coops et al. (2007) also found good correlations between field and LiDAR-derived mean and maximum tree height estimates for Douglas fir (*Pseudotsuga menziessii* (Mirb.) Franco) and western hemlock (*Tsuga heterophylla*) plots on the east coast of Vancouver Island, Canada ($R^2 = 0.85$, $P < 0.001$, SE = 1.8 m; and $R^2 = 0.82$, $P < 0.05$, SE = 2.2 m, respectively). Holmgren et al. (2003) retrieved basal area weighted mean tree height and stem volume from gridded laser scanning data using regression models and investigated the effect of scanning angle on basal area weighted mean tree height estimates and crown coverage. The dominating tree species in that study were Norway spruce, Scots pine (*Pinus sylvestris* L.), and birch (*Betula* sp.). On average, 90% of the variation in basal area weighted mean tree height was explained using linear regression equations. The RMSE values ranged between 1.45 and 1.56 m (10–11% of average height). The scanning angle had no significant impact on estimates of basal area weighted mean tree height. Wezyk et al. (2008) found $R^2 = 0.8$ when comparing airborne tree height estimates obtained from a CHM against field inventory data and—on average—underestimates in the order of 0.1–0.9 m (SD = 1.8 m), depending on whether maxima of raw LiDAR were used instead of smoothed CHM heights. In forests dominated by Norway spruce and Scots pine in southeast Norway, Næsset (2009a) determined Lorey's mean height with RMSE ranging between 0.81 and 0.93 m for a variety of LiDAR instruments and acquisition parameters.

Canopy height models

LiDAR retrieved canopy heights can be presented in a so-called canopy height model (CHM) that presents the height of the canopy as a 3D georeferenced surface. CHMs represent stand-level canopy heights; however, individual trees and tree crowns may be delineated from CHMs with

varying levels of success (Nelson et al. 2000; Brandtberg et al. 2003; Weinacker et al. 2004) using multi-scale moving window operations (Popescu and Wynne 2004), valley following approaches (Gougeon 2005), or watershed algorithms (Chen et al. 2006). As CHMs are typically derived from first LiDAR returns, suppressed trees are not represented. Lee and Lucas (2007) presented and validated the height-scaled crown openness index (HSCOI) to detect suppressed trees and improve estimates of stocking density. The method was tested in mixed species woodlands and open forests in Queensland, Australia, and the method yielded reliable outcomes with regard to tree height retrieval ($R^2 = 0.81$) as well as identifying individual trees, and tree stocking ($R^2 = 0.82$). Van Leeuwen et al. (2010) have used a modified Hough transform to fit crown shapes to the raw LiDAR point cloud that allows creation of a canopy model in which single trees are represented as individual objects from which crown delineations can easily be derived through geometric operations.

Individual tree height estimates

Individual tree heights can be retrieved after a segmentation step where individual trees are isolated in the point cloud (Pfeifer and Briese 2007). Besides crown delineation from CHMs, raw LiDAR point cloud data have been used for segmentation directly. Morsdorf et al. (2004) used raw LiDAR data (x, y, z triplets) to identify individual trees through k-means clustering. The seed points set for this cluster analysis were taken from the local maxima in the digital surface model (DSM) that was derived using a smoothing filter, and a morphological moving window operation. Reitberger et al. (2008, 2009) used normalized cuts to segment individual tree crowns in the LiDAR point cloud data. The normalized cut has been presented by Shi and Malik (2000) as an algorithm for image segmentation that maximizes dissimilarity between the segmented groups and similarity within groups. Following this approach, point clouds are gridded to voxel space and are presented as graphs with edges between every pair of nodes. Edges are weighted based on internode distance and similarities in LiDAR return intensity values. Segmentation is then achieved by finding those edges that minimize the sum of weights between every node in A to every node in B, with A and B being segments.

Estimates of tree height have been made with reasonable accuracy and typically show underestimation compared to field observation. Morsdorf et al. (2004) used an extremely high density (>30 p m^{-2}) LiDAR data set representing a test area in the Swiss National Park containing mostly mountain pine (*Pinus montana* ssp. *arborea*) and some stone pine (*Pinus cembra*), ranging in age between 90 and 200 years and heights ranging roughly between 9 and 15 m. Linear regression on tree height measurements yielded an adjusted $R^2 = 0.92$ and RMSE = 0.6 m; however, it was noted that their clustering algorithm did not succeed in identifying all trees present in the test site and outliers were weighted to reduce their influence on the fit or were removed. Of the approximately 2,000 trees present, only 1,200 clusters were identified, which was ascribed to the high stocking density of *Pinus* sp. in the test area. Næsset and Økland (2002) retrieved tree height accurately with a standard deviation of 3.15 m (and $R^2 = 0.75$), compared against ground truth measurements. Tree height was estimated using the natural logarithm of maximum return height of the first echo as dependent variable. Heurich (2008) estimated tree height among 1,100 LiDAR measured, deciduous and coniferous trees and found underestimates in tree height were somewhat lower for deciduous species (−0.43 m) than coniferous trees (−0.63 m) and larger on slopes and valleys (−0.85 m) than on high lands (0.17 m). Standard deviations were circa 1.4 m but were smaller on high altitude areas (0.9 m) than on slopes and in valleys (1.6 m). Linear regression against field measurements yielded high $R^2 \geq 0.97$. Compared to plot-based estimates, individual tree height estimates have been shown to improve stand level volume and growth estimates. Yu et al. (2008) compared three different techniques for estimating mean height and volume increments from LiDAR data acquired over consecutive years. Temporal change in plot-based percentile heights, DSM heights, and individual tree heights were compared and it was found that individual tree maps best explained height increments. Table 1 shows an overview of LiDAR-derived tree height estimates and their accuracies.

LAI and fractional cover

Leaf area index (LAI) and fractional cover estimates are of great importance to many forest-monitoring applications; for forest growth modelling and fire risk assessments, just to mention a few (Jupp et al. 2009). LAI is defined as the maximum projected leaf area per unit ground surface area (Myneni et al. 1997) and being a ratio of surfaces, it is a dimensionless quantity. Fractional cover is defined as the projection of the tree crowns onto the ground divided by ground surface area. Morsdorf et al. (2006) investigated the potential of discrete return, small footprint airborne LiDAR to estimate fractional cover and leaf area index. The leaf area index was estimated using a proxy based on contact frequency of the first, last, and single LiDAR returns.[1] A regression of LiDAR-derived LAI estimates against hemispherical LAI estimates yielded an R^2 of 0.69 and an

[1] The term 'single returns' was used to refer to the occasion that only one echo was sensed, and hence no distinction in order can be made.

Table 1 Overview of LiDAR-derived tree height estimates and their accuracies

Reference	Species/location	Plot level				Individual level	Results
		Lorey's mean height	Mean tree height	Max. height	Basal area weighted mean tree height	Tree height	
Næsset and Økland (2002)	Dominating Norway spruce	✔				✔	$\delta = 1.49$ m; $R^2 = 0.91$ and $\delta = 3.15$ m; $R^2 = 0.75$, resp.
Andersen et al. (2005)	Western Washington State, US	✔					$\Delta = 1.5$ m; $R^2 = 0.98$
Coops et al. (2007)	Douglas fir and western hemlock		✔	✔			$R^2 = 0.85$; SE = 1.8 m and $R^2 = 0.82$; SE = 2.2 m, resp.
Holmgren et al. (2003)	Norway spruce, Scots pine, birch				✔		$R^2 = 0.90$; RMSE = 1.45–1.56 m
Morsdorf et al. (2004)	Mountain pine, stone pine					✔	$R^2 = 0.92$; RMSE = 0.6 m
Lee and Lucas (2007)	Queensland, Australia					✔	$R^2 = 0.81$
Næsset (2009a, b)	Dominating Norway spruce	✔					$R^2 = 0.81$–0.93
Wezyk et al. (2008)	Central-west Poland					✔	$R^2 = 0.8$; $\delta = 1.8$ m
Heurich (2008)	Bavarian Forest NP, Germany					✔	$R^2 = 0.97$–0.98

RMSE of 0.01. Fractional cover was also estimated and was taken from the ratio of first LiDAR returns echoed from vegetation and the total amount of first LiDAR returns and showed a slightly higher fraction of explained variation, $R^2 = 0.73$, with a RMSE of 0.18. The study was conducted in a boreal pine forest in Switzerland, dominated by mountain pine and some stone pine. Riaño et al. (2003) calculated fractional cover as the fraction of total canopy surface hits in relation to the total number of hits, but they did not state accuracies of retrieval. In a study conducted by Lefsky et al. (2005b), LAI was retrieved using SLICER data with an R^2 of 0.81, for a wide variety of forest types and growth conditions in the Pacific Northwest of the USA, using stepwise regression techniques on canonical variables derived from the LiDAR data. These canonical variables are linear combinations of a set of original LiDAR data variables, such that the independent canonical variable, or set of canonical variables, maximizes the explained variance in the target variable, here LAI. Despite the high LAI values found in the study area (mean = 6.45), no asymptotic behaviour in the regression for LAI was found. This may indicate potential of LiDAR techniques to overcome saturation problems often encountered with other means of remote sensing, such as radiative transfer modelling using hyperspectral remote sensing, or using spectral indices. Sasaki et al. (2008) estimated LAI and gap fraction (complement of fractional cover) from airborne LiDAR and compared these estimates against vegetation indices obtained from hyperspectral data. The fraction of ground returns relative to total number of first and single returns was a highly significant estimator for both canopy parameters, with $R^2 > 0.77$ (for both LAI and canopy openness) and RMSE = 0.24 and 0.033 for LAI and canopy openness, respectively. Moreover, this LiDAR statistic was a good estimator even at point densities below 1 m^{-2}. Zhao and Popescu (2009) used LiDAR-derived LAI estimates to validate an optical satellite LAI product. The authors used normalized height metrics and metrics related to the laser penetration depth and found that the latter explained hemi-photo LAI estimates best, in analogy with the Beer's law that is used to obtain the ground estimates of LAI. Correlations with ground truth were dependent on plot size of extracted LiDAR metrics and it was found that a radial plot size of 25 m yielded the best correlations.

Canopy height profiles

In addition to leaf area index, another variable has been introduced in forestry to describe the foliage structure: the foliage height profile. This quantity describes the vertical distribution of leaf material throughout the canopy and was first developed by MacArthur and Horn (1969). To account for the inability of LiDAR remote sensing to discern branches from leaf material, the phrase canopy height profile (CHP) or sometimes apparent foliage height profile is often used (Coops et al. 2007). Derivation of canopy

height profile from LiDAR data has first been demonstrated by Lefsky et al. (1999) for large footprint, full-waveform LiDAR data and was later derived for small footprint, discrete return LiDAR by Riaño et al. (2003). Integration of the CHP over the canopy height yields the apparent leaf area index, but does not account for foliage clumping. Coops et al. (2007) found reasonable good correspondence between field- and LiDAR-derived apparent foliage profiles, but noted that LiDAR-derived CHPs are biased towards the top of the canopy, whereas ground-based methods are biased towards the lower strata in the canopy. In addition, the methods applied did not account for more complex multi-layered canopy structures, resulting in a further bias between the field and airborne techniques. To overcome such complications of multi-layering in forest canopies, Zimble et al. (2003) investigated the use of airborne LiDAR for the classification of single- and multi-story forests. The results suggested strongly that LiDAR-derived data could be used to distinguish between these two vertical forest types. The coefficient of variation (CV) was used to reveal gradients of diversity and canopy complexity. Higher values for CV corresponded to more diverse multi-story areas, whereas low values represented thinned, single story areas. Classification of forest stands based on their canopy strata (single-story or multi-story) resulted in an overall classification accuracy of 97%, with an overall kappa statistic of 0.89, indicating that the technique proved successful in mapping forest canopy layering accurately at a landscape scale. The difficulty relating to the detection of tree crowns from suppressed small trees in the forest stand was addressed by Maltamo et al. (2004) in southern Finland, who made use of theoretical distribution functions to describe the occurrence of small and suppressed trees to improve the accuracy of canopy height profiles and, subsequently, stand volume estimates.

Biomass and tree volume

In the study conducted by Lefsky et al. (2005b), above-ground biomass was retrieved from airborne LiDAR data with an adjusted R^2 of 92%. Use was made of regression techniques on canonical variables. This methodology was similar to the methods which were applied in the same study to retrieve LAI, as described previously in this article. Drake et al. (2002) evaluated four different LiDAR metrics in their capacity to estimate forest structural parameters in the La Selva Biological Station, a tropical wet forest site in Costa Rica. The metrics used were canopy height, height of median energy, proportional amount of ground returns, and the ratio of median energy height and canopy height. The LiDAR data were acquired using the LVIS instrument emulating acquisition characteristics resembling those of the—then proposed—VCL mission.[2] Variance in the above-ground biomass was best explained by the height of median energy metric, with an R^2 of 53% for footprint estimates. Multiple-term regression explained distinctively more of the variation than the single-term equation. The best estimates were obtained at a plot size that exceeded the size of one footprint, rather than at the level of individual LiDAR footprints. This was thought to result from an averaging effect from larger samples and geo-location errors in relating individual footprints to ground sample measurements. Using multiple-term regression on the height of median energy (i.e. the same metric used in two terms), above-ground biomass at plot level was explained up to 93% of the encountered variation, with a RMSE of 18.39 Mg ha^{-1}. Other approaches were used by Riaño et al. (2003), where total biomass was estimated using a linear regression on the mean height of all laser pulses, but an accuracy assessment of the procedure was not given, and by Lefsky et al. (2005a), where above-ground biomass was estimated from maximum canopy height squared, again using linear regression ($R^2 = 73\%$, and RMSE = 58.3 M-g ha^{-1}) for a tropical, relatively undisturbed old-growth forest within the Amazon basin, Brazil. Anderson et al. (2008) found great improvement in estimating above-ground biomass for mixed species forests (hardwood, soft-wood) in Northern temperate forests in the USA using stepwise linear regression on lower order, minimum noise fraction (MNF) transformed (Green et al. 1988) AVIRIS data and co-registered LiDAR (LVIS) percentile heights. The AVIRIS metrics explained most of the variance, but percentile heights from LVIS data significantly increased explained variation and lowered uncertainty in the estimates. About 25% more variation in above-ground biomass was explained by combining AVIRIS data with LVIS data for unmanaged forests, while error levels decreased by 25%. For managed forests, the increase in R^2 and decrease in error of prediction was much lower, about 8–9% and 5–8%, respectively. Overall, despite this improvement in estimation, above-ground biomass (irrespective of species and management) was still relatively poorly estimated, with R^2 ranging between 0.39 and 0.55. For single species stands, biomass estimates were best retrieved using AVIRIS data alone. In the southeastern US, Popescu et al. (2003) utilized LiDAR estimates of crown width to derive biomass estimates via linear regression techniques. Crown diameter alone was able to explain up to 83% of the variance associated with tree volume. Without the use of crown diameter estimates and based on LiDAR height measures only, the decrease in R^2 was on average 0.09, but this was considerably higher for deciduous trees (maximum decrease in R^2 of 0.25). Crown diameter estimates also improved regression

[2] The VCL (Vegetation Canopy LiDAR) Mission was intended for terrestrial ecosystem and climate modelling and prediction.

estimates of biomass, on average the increase in R^2 was 0.11, with a maximum of 0.24 for deciduous plots. The maximum R^2 value for biomass estimates in deciduous stands was still low, $R^2 = 0.33$, and RMSE of 44.41 Mg ha^{-1}. Maximum explained variance was found for pine stands, where the average crown diameter alone explained 78% of the variance in biomass. Maltamo et al. (2004) showed that predictions of small and suppressed trees can be obtained from fitted Weibull distributions to increase the accuracy of timber volume estimates and showed that RMSE values decreased from 25 to 16%. Næsset et al. (2005) retrieved timber volume estimates with standard deviations of the difference between predicted values and ground truth in the range 8.3–14.9% of mean ground reference values. Yu et al. (2008) estimated stand volume growth best from statistics obtained from the difference between DSMs obtained from LiDAR data acquired from 2 years and resulted in an adj. $R^2 = 0.57$ and standard deviation of 8.39 m^3 ha^{-1}; however, a better correlation was found when plot-based percentile heights and mean height of individually identified trees were included in the regression equation (adj. $R^2 = 0.75$ and $\delta = 6.7$ m^3 ha^{-1}). Heurich (2008) was able to estimate timber volume from coniferous trees in Germany with $R^2 = 0.87$–0.95 and $CV_{RMS} \leq 35\%$ using crown diameter and tree height as explanatory variables. Timber volumes were more accurately determined for coniferous trees than for deciduous species. Næsset and Gobakken (2008) estimated above- and below-ground biomass across different regions within the boreal zone in Norway using point densities varying between 0.7 and 1.2 m^{-2}. Estimates were obtained using canopy height and canopy density as explanatory variables and explained variations of biomass ranged between 85 and 88%. Geographical region, included as a dummy variable, accounted for 32–38% variation. Through sensitivity analysis it was shown that the proportion of species has a large impact on biomass estimates and a 1% increase in the proportion of spruce increased biomass estimates by 0.2–0.3%. The researchers therefore deemed local variability a critical issue and recommended that sample plots, needed to calibrate the LiDAR regression equations, are distributed throughout the entire area of LiDAR acquisition to account for (sub-)regional differences. Breidenbach et al. (2010) found improved accuracy and precision of timber volume estimates (RMSE = 34.56 m^{-3} ha^{-1} or 17.07% of mean volume) using fused multispectral and LiDAR data by clustering trees and groups of trees standing closely together using the iterative closest point algorithm and calculating stand level volume estimates from the sum of clusters rather than area-based estimates. For clusters found in the LiDAR data for which no field data were obtained, volume estimates were imputed based on similarity with neighbouring clusters for which corresponding field observations were available. Crown volume was estimated from various coniferous and deciduous species in the northwest of the USA by Kato et al. (2009) through a wrapping procedure that was based on a 2D convex hull algorithm. Crown volume estimates were compared against total station measurements showing a significant match. The procedure further allowed for retrieval of tree parameters from the wrapped tree crowns. A summary of LiDAR-derived forest metrics and their accuracies is provided in Table 2.

Species classification

LiDAR remote sensing is increasingly used for the classification of tree species based on the spatial configuration of LiDAR returns in the point cloud and LiDAR intensity values. The use of intensity values from LiDAR returns is an area of much research and currently no standard procedures exist for radiometric calibration of LiDAR data (Ørka et al. 2009; Wagner et al. 2008). Over forest areas, differences in intensity values may be observed as a result of variations in laser path length, beam divergence, scan angle, sensor characteristics, attenuation of light by the atmosphere, orientation of leaves and branch facets, and topography (Donoghue et al. 2007). These difficulties limit the validity of classification rules among study areas and among the different LiDAR instruments and acquisition parameters used.

Despite difficulties related to the radiometric calibration of LiDAR data, intensity values have successfully been used for species classification. Holmgren and Persson (2004) showed that Norway spruce and Scots pine can be classified with an overall accuracy of 95% using discrete LiDAR data. Individual trees were segmented first and species were classified based on statistics of the 3D spatial arrangement and intensity values of the segmented point clouds. Reitberger et al. (2009) have applied supervised and unsupervised classification to classify spruce and fir from full waveform LiDAR data and used the 3D point configuration, intensity values, the number of returns per waveform, and pulse width. Classification accuracies were obtained up to approximately 95%. Ørka et al. (2009) compared various structural and intensity LiDAR statistics to classify birch and spruce in southeast Norway. It was shown that the significance of these LiDAR features differed among echo categories (first, single, and last return). In this study, individual trees were not segmented but statistics were obtained within a radial distance from tree tops, with radii based on field determined average crown size. To account for variation of LiDAR statistics obtained from trees of different age and height, LiDAR returns were normalized to field-measured tree height and to penetration depth into the tree crown. It was found that the normalized height values were of little value in the classification of tree species; however, coefficient of variation of normalized return heights and skewness and kurtosis of the return distribution

Table 2 Overview of LiDAR-derived forest metrics and their accuracies

Reference	Species/location	LAI	fcover	AGBM	Above & below ground biomass	Timber volume	Mean DBH	QMSD	Results
Morsdorf et al. (2006)	Mountain pine, stone pine	✔	✔						$R^2 = 0.69$; RMSE = 0.01 and $R^2 = 0.73$; RMSE = 0.18 resp.
Lefsky et al. (2005b)	Pacific Northwest US	✔		✔			✔		$R^2 = 0.81$ and $R^2 = 0.92$ and adj. $R^2 = 0.65$ resp.
Drake et al. (2002)	La Selva, Costa Rica			✔				✔	$R^2 = 0.93$; RMSE = 18.39 Mg ha^{-1} and $R^2 = 0.77$–0.93 resp.
Lefsky et al. (2005a)	Amazon basin, Brazil			✔					$R^2 = 0.73$; RMSE = 58.3 Mg ha^{-1}
Anderson et al. (2008)	Northern temperate forest, US			✔				✔	$R^2 = 0.39$–0.55 and adj. $R^2 = 0.25$–0.33, resp.
Popescu et al. (2003)	Southeast US			✔					$R^2 = 0.33$; RMSE = 44.41 Mg ha^{-1}
Næsset et al. (2005)	Norway spruce, Scots pine					✔	✔		$\Delta = 8.3$–14.9% of mean and $\delta = 5.5$–15.8% resp.
Yu et al. (2008)	Kalkinnen, Finland					✔			$R^2 = 0.75$ and $\delta = 6.7$ m^3 ha^{-1}
Heurich (2008)	Bavarian Forest NP, Germany					✔			$R^2 = 0.87$–0.95 and $CV_{rms} \leq 35\%$
Næsset and Gobakken (2008)	Southeast Norway				✔				$R^2 = 0.85$–0.88
Breidenbach et al. (2010)	Southeast Norway					✔			RMSE = 34.56 m^3 ha^{-1}

LAI leaf area index, *fcover* fractional cover, *AGBN* above-ground biomass, *Mean DBH* mean diameter at breast height, *QMSD* quadratic mean stem diameter

were found significant depending on whether first, last, or single returns were used. In addition, maximum and mean intensity values related significantly to tree species. Donoghue et al. (2007) found LiDAR intensity the single best estimator for determining fractional composition of the species lodgepole pine (*Pinus contorta*) and sitka spruce in west Scotland, but noted that noise was present in the intensity data that was likely due to topographic effects. Coefficient of variation (CV) and mean height were also identified as useful estimators to retrieve proportions of spruce. Mean height was not used to classify species, but to identify gaps and variability in canopy height and, as such, it improved proportion estimates of spruce. Improvement in classification of tree species and the use of LiDAR intensity values may also be gained through multi-band LiDAR systems; the development of which is currently a topic of investigation (Morsdorf et al. 2009).

Other tree structural quantities

Diameter at breast height (DBH) is a critical forest inventory parameter of paramount importance in deriving estimates of biomass, timber volume, and forest growth, to mention just a few. Lefsky et al. (2005b) retrieved mean stand DBH with an adjusted R^2 of 0.65 for the forest stands mentioned earlier in the Pacific Northwest of the US. Drake et al. (2002) derived quadratic mean stem diameters from LVIS LiDAR data, through stepwise multiple regression, for a tropical wet forest site, La Selva Biological Station, Costa Rica, yielding an explained variation of 77%, for footprint-level estimates and 93% for plot-level estimates. Anderson et al. (2008) obtained considerably lower R^2 values for quadratic mean stem diameter from LVIS data alone, or in combination with AVIRIS data (adj. $R^2 = 0.25$–0.33 with PRESS RMSE = 2.61–3.00 cm) in the Barlett Experimental Forest within the White Mountain National Forest, north-central New Hampshire. Næsset et al. (2005) achieved standard deviations of 5.5–15.8% for differences between LiDAR-predicted mean stem diameter and corresponding ground truth values. These studies typically use tree height, crown width, percentile estimates, and canopy density estimates to infer stem diameter. These and other LiDAR-derived metrics have been summarized in Table 2, together with their accuracies. As can be seen

from these studies, the accuracy by which DBH is estimated varies widely, and much comes down to spatially confined calibrations of LiDAR metrics to estimate DBH. No regression equation can be applied generically over different forest types and regions of the world, and a more straightforward means for obtaining DBH values through the use of LiDAR technology is provided by ground-based laser scanning.

In contrast to the Euclidean measures typically included in forest inventories, some studies have investigated the use of LiDAR-derived metrics for multifractal analysis. Drake and Weishampel (2000) compared multifractal measures derived from field-based work and LiDAR scans of a longleaf pine (*Pinus palustris*) savanna. The derived metrics showed good agreement within sites, whereas multifractals for different sites were clearly distinct. This indicates that different abiotic processes cause different fractal dimensions and—through future research—this may be used to identify abiotic processes driving forest growth. The significance of fractal analysis to forestry, to better understand the underlying ecological and abiotic mechanisms, has also been formulated by, e.g. Boudon et al. (2006) and Alados et al. (1999).

Influence of scanning exterior orientation parameters

Retrieval of biophysical parameters from LiDAR data may depend on sensor and acquisition characteristics and care should be taken in the interpretation of LiDAR metrics obtained from different scanners for use in retrieving biophysical parameters (Næsset 2009a). Lovell et al. (2005) investigated the effect of airborne LiDAR scanning (ALS) parameters on retrieving tree height estimates at the plot level, using simulated LiDAR data from simulated plantations and found that the retrieved predominant height was linearly related to the mean nearest neighbour spacing between the LiDAR point samples. A similar linear relationship was obtained from actual LiDAR data from field measured plots (9-year-old *P. radiata*). Both simulated and actual data sets showed that LiDAR-derived predominant tree height underestimates actual predominant tree height, but using the actual data, this effect was less severe than using the simulations. The difference in predominant height estimates between actual ALS data and field measurements was 2 m using an average point spacing of 1.04 m. Besides the effect of point spacing, the footprint size was found to be of influence on the retrieved predominant tree height, but its effect was not investigated. Goodwin et al. (2006) investigated the effect of platform altitude (1,000, 2,000 and 3,000 m), scan angle (10 and 15 degrees), and footprint size (0.2, 0.4 and 0.6 m) on the retrieval of canopy height profile, crown volume, tree height, and the fraction of ground returns from Australian sclerophyll forests. The retrieved canopy height profiles showed no significant influence from increasing platform altitudes or increasing footprint sizes, whereas the individual tree attributes crown area and volume were strongly affected by point spacing. This effect was different for the various structural stand characteristics included in the study. Increased platform altitudes considerably reduced the fraction of ground returns. However, in contrast to Lovell et al. (2005), no significant differences in tree height estimates were observed for the various platform altitudes. The large crown area and high crown cover contained in the study were given as the reason for this. It was emphasized that smaller crown areas result in fewer LiDAR returns per tree and hence, greater uncertainty in estimating tree level parameters. Similar research was conducted by Yu et al. (2004) for forests comprising mainly Scots pine, Norway spruce, and birch. The test sites were located in southern Finland, and the study was conducted for ranges in flight altitudes (400, 800 and 1,500 m), point spacing (10, 5 and 2.5 points m^{-2}), and footprint sizes (0.2, 0.4 and 0.75 m). Estimates of tree height and stocking were affected by flight altitude, but all retrievals were considered of relative high accuracy (up to approximately 0.5 m bias). The underestimation of tree height was more profound for coniferous species than for birch species. Pulse density was found to have a greater effect than footprint size on the bias and standard deviation for tree height and tree stocking. Birch height estimates were again less influenced by varying footprint size. A considerably greater impact of footprint size on biases and errors in tree height estimates was encountered for large footprint size (>1 m) LiDAR inventories (Roberts 1998; in Goodwin et al. 2006), where it was demonstrated that increasing the footprint size from 5 to 25 m improved tree height estimation. Holmgren et al. (2003) investigated the effect of scanning angle on basal area weighted mean tree height estimates, but found no significant impacts. In comparison to Goodwin et al. (2006), Morsdorf et al. (2008) found a somewhat larger underestimate of tree height with increasing flying altitude (900 vs. 500 m), and found an overestimation of LAI (0.29 m) at 900 m and a slight underestimation (0.06) at 500 m. Fractional cover decreased with increasing flying height. A larger number of last returns were recorded from inside the forest canopy with increasing flying altitude. This was explained to result from the larger footprint and may explain errors in LAI and fractional cover since these parameters were derived from relative frequencies of first, last, and single echoes. With increasing flight altitude, also an increase in distance between first and last pulse was observed and a suggestion was made that the sensor capacity to distinguish individual returns decreases when intensity values decrease as a result of increased flying height. We anticipate that additional multi-scattering caused by the wider footprint may further reduce the detection of discrete

returns as it causes the returned energy to spread out over time-of-flight. Despite the found error margins, the authors concluded that tree height, fractional cover, and LAI were found within tolerable ranges for a flying altitude of 900 m using regression models correctly calibrated for this altitude. Næsset (2009a) compared height metrics and biophysical parameters among data obtained from different scanners flown over one study area. Data from different scanners showed that biophysical parameters could be retrieved with appreciable precision; however, among scanners, different biases in estimates were observed. It was found that first, last, and single returns are affected by flying height (higher values at higher altitudes) and increasing pulse repetition rate (PRR) tends to produce canopy height distributions that are shifted upwards. Upward shifted height distributions are a result of higher single and first returns and fewer last returns. A clear cause for this was not found but it was hypothesized that higher repetition rates result in lower pulse energies per emitted pulse and smaller penetrative capacity.

Influence of terrain slope

Besides the scanner's exterior orientation parameters during acquisition, terrain slope influences tree height estimates. In cases where terrain elevation differences within the LiDAR footprint are large, tree height estimates can be difficult to retrieve due to the ambiguous cause of variation in canopy height—either terrain elevation or tree height. Takahashi et al. (2005) investigated the effect of terrain slope and roughness on the capacity of small footprint LiDAR to retrieve tree height for middle-aged (48-year-old) sugi (*Cryptomeria japonica* D. Don) plantations in mountainous regions in Japan. The accuracy by which individual tree heights could be detected correctly was 74% for steep slopes (37.6° ± 5.8° SD), 86% for gentle slopes (15.6° ± 3.7° SD), and 92% for gentle sloping yet rough terrain (16.8° ± 7.8° SD). Respective average errors (bias) between field measured and LiDAR-derived tree height estimates were 0.227, −0.473, and −0.183 m, with corresponding RMSE values of 0.901, 0.846, and 0.576 m, respectively. The relatively greater underestimation of tree height on the gentle slope, compared to on the gentle sloping yet rough terrain, was thought to be due to the higher percentage of first LiDAR returns on these plots and the increased likelihood therefore to sample tree tops. The overestimation of tree height on the steep slope was likely due to trees leaning towards the valley side of the slope, which causes the distance from tree top to orthogonal point on the ground to exceed the actual tree height. On the contrary, Heurich (2008) found larger underestimates on slopes and in valleys for individual height estimates from coniferous trees in southeast Germany. Morsdorf et al. (2008) found no dependence of fractional cover or LAI estimates on terrain slope, but noted somewhat larger height underestimates as a result of increasing incident angle.

Generality of LiDAR estimates

Many studies have used LiDAR indices to estimate stand structural attributes, using regression equations. However, few studies have investigated the generality of such regression equations over a variety of environmental conditions. Lefsky et al. (2005b) studied the capacity of regression techniques using LiDAR indices from SLICER data to estimate 17 structural characteristics over a wide range of environmental conditions in the Temperate Coniferous Needleleaf biome in the Pacific Northwest of the USA. Included tree species were Douglas fir, western hemlock, and Sitka spruce (*Picea sitchensis*). The structural characteristics included in the study covered a wide range of tree height, canopy height, volume-related quantities, and LAI. The derived regression equations showed a general validity over the test sites. Incorporation of knowledge on environmental conditions into the regression equations proved only helpful for estimates of DBH_{max} (maximum DBH encountered) and stem density. Whereas these findings are only preliminary results for testing the generality of these regression equations over the various environmental conditions one could encounter, the question was raised whether or not "in forests dominated by coniferous species, tree architecture is constrained to the point where a unified relationship between LiDAR measurements and stand structure might exist for these forests generally" (Lefsky et al. 2005b). However, recent research by Næsset and Gobakken (2008) on biomass mapping shows that field observations are needed from plots located throughout the entire study area.

Spaceborne LiDAR

Spaceborne LiDAR acquisition is currently possible from the ICESat satellite and its mounted instrument, the geoscience laser altimeter system (GLAS). Compared to airborne LiDAR, fewer studies have been conducted on the use of GLAS data for forest inventory purposes, but its launch and the study of its data are of paramount importance to future LiDAR missions (Nelson 2008). The GLAS instrument has been in orbit since January 2003 and has provided a chronologically discontinuous set of global LiDAR data since. GLAS is mainly intended for scientific studies on ice-sheet thickness, cloud and atmospheric properties, and land elevations. It returns a full waveform and thus enables the retrieval of backscatter profiles. The

instrument has a 120 m × 60 m ellipsoid footprint with a spacing of 175 m along its track (Ranson et al. 2004a) and a 183-day repeat cycle. Sun et al. (2008) evaluated the spatial accuracy and the quality of waveform recording of the GLAS instrument. The location accuracy of the GLAS footprints was evaluated by comparing the elevation profiles with an SRTM (Shuttle Radar Topography Mission) derived 60 m DEM. These DEMs are obtained from radar data acquired from the Endeavour Space Shuttle. Maximum correlation between the sets was found by shifting the GLAS transect data within 1 or 2 pixel distances from the original locations. Of special interest with regard to the derivation of forest attributes and forest surface classification is the GLA14 product that is automatically derived for the GLAS satellite data (e.g. Harding and Carabajal 2005). This product contains the decomposition of up to six Gaussian distributions, describing the received GLAS waveform.

Tree height

The retrieval of height estimates from GLAS waveform data requires specific attention to mitigate the effects of terrain elevation, in case of profound ruggedness. With the large footprint size of GLAS data, the elevation differences that are present within the footprint can be substantial in comparison with the predominant tree height and make accurate tree height estimates more difficult than with small footprint LiDAR. Yong et al. (2006) investigated this effect of terrain slope on tree height estimates from simulated large footprint LiDAR data and compared the simulation results with data from the GLAS instrument. The simulations were consistent with GLAS data in that the waveform length elongates and the waveform peaks and front slope angle decrease in magnitude as the terrain slope increases. However, the relationship between waveform length and terrain slope was found to be near linear, which indicates that these terrain effects can be corrected for. Lefsky et al. (2005a) attempted to estimate forest biomass, via maximum canopy height estimates derived from GLAS data, for different sites across the USA (Oregon and Tennessee) and the Amazon. The tree species included in the study comprise a wide variety of coniferous and hardwood species. The maximum canopy height was estimated with regression equations using waveform extent and a terrain index as independent variables. The terrain index was similar in concept to what was used by Yong et al. (2006). The R^2 of the maximum tree height regression varied from 59 to 68% for the different sites under investigation, and RMSE varied from 4.85 to 12.66 m. A study conducted by Rosette et al. (2008) on trees in a mixed temperate forest located in Gloucestershire, UK, yielded higher explained variation following a similar regression analysis. The study comprised Norway spruce, Douglas fir, Scots pine, Corsican pine (*Pinus nigra* var. *maritima*), Japanese larch (*Larix kaempferi*), and common alder (*Alnus glutinosa*). Estimates of maximum tree height derived from waveform extent (WE) and a terrain index (TI) produced an R^2 of 0.90 and a RMSE of 2.86 m. This regression, similar to the one used by Lefsky et al. (2005a), explained more variation than results from Lefsky et al. (2005a). Whereas these studies required the use of a DEM to quantify the terrain's slope, Lefsky et al. (2007) attempted to describe the terrain's slope based on a trailing edge effect that occurs in the waveform data, which is caused by, and correlates with, terrain slope, and therefore eliminates the need for a DEM. The algorithm estimated canopy height with a RMSE of 5 m ($R^2 = 0.83$) for evergreen conifer, deciduous broadleaved, and mixed stands in North America, and tropical evergreen broadleaf forests in Brazil. Since GLAS data do not fully cover the Earth's surface, it has been used for calibration purposes of other remote sensing data with a (near) global coverage. An example of this is given in a study conducted by Simard et al. (2008) where average heights of mangrove trees along part of the coast of Colombia were estimated using SRTM data, version 2. SRTM (Shuttle Radar Topography Mission) version 2 data are a near global coverage of the Earth's topography, collected using radar interferometry from the Space Shuttle Endeavour. The GLAS data were used to calibrate SRTM data in this study.

Land cover classification and disturbance detection

GLAS waveform data have also been investigated for use in supporting land classification processes and the detection of forest disturbances, and this research has been relatively successful. Ranson et al. (2004a) used descriptive measures of GLAS waveforms that were obtained from a range of different land cover types in central Siberia. The waveforms were described by their signal length, front slope angle, and energy ratio. Compared to MODIS land cover data, the GLAS data proved more useful in distinguishing abandoned fields or clear cuts with early stage regeneration within deciduous forests. Although the ranges that were found for the various descriptive measures exhibited a large degree of overlap for the different land cover types due to natural variation within each cover type, the results indicated the usefulness of these descriptive measures in supporting land cover classification. Similar research with respect to disturbances was conducted by Ranson et al. (2004b). Here, the application of GLAS waveforms for identifying disturbed forests was studied, by comparing waveforms from healthy forests with those from insect damaged forests, and from recently fire damaged forests. The results showed that fire-damaged stands are characterized by lower waveform heights and larger front slope angles, indicating a greater influence from ground

returns in the waveform. Insect-damaged stands exhibit a waveform height and front slope similar to undamaged stands. Whereas not specifically mentioned in the article, no forest type was found for which the range of descriptive measures was significantly distinct from those of other forest types.

Timber volume and biomass

An indirect use of relating descriptive measures of the LiDAR waveform to forest structural characteristics was investigated by Ranson et al. (2007), who used neural networks to infer timber volume from GLAS data for a range of canopy densities and forest types in central Siberia. The best neural network found was based on the waveform centroid, and the heights of the 100, 50, and 25% quartiles relative to ground peak (i.e. H100, H50, H25, respectively). This neural network explained 68% of variation with an RMSE of 99 m^3 ha^{-1}. The mean timber volume that was thus found for a 10° by 12° area in Central Siberia was compared against earlier ground-based findings and this revealed that the difference was less than 5%. A study conducted on the use of GLAS data for biomass estimation was carried out by Sun et al. (2008), who showed that the correlation between GLAS 75%-quartiles (i.e. heights of the 75%-quartile) and aggregated coincident LVIS quartiles revealed an R^2 of 0.82 for LVIS 75%-quartiles and an $R^2 = 0.83$ for LVIS 50%-quartiles. In an earlier study, conducted by Drake et al. (2002), the 50%-quartile in LVIS data proved to be highly correlated with forest biomass. This suggests good potential of GLAS data for biomass retrievals. An overview of GLAS-derived forest metrics and related accuracies are provided in Table 3.

Terrestrial laser scanning

Complementary to the airborne and spaceborne LiDAR technologies described above is terrestrial laser scanning (TLS). This technology offers the capacity to map 3D surfaces with millimetre accuracy. The many algorithms that have been developed over the past decades allow a variety of surface types to be modelled accurately and with great precision. Having been developed mainly for purposes in mechanical engineering, for tasks such as deformation analysis and reverse engineering, the technology has made great advancements over a short time span. With the aid of terrestrial laser scanning, it is now possible to describe architectural constructs, factory halls, human and animal anatomy, facial expressions, and a range of other 3D shapes in a digital format for subsequent computer processing. Terrestrial laser scanning is able to accurately assess timber reserves and to acquire inventory parameters in an unequivocal, objective, and reproducible manner. Recent studies have explored the use of TLS for tree reconstruction for use in a number of tree physiological studies (Côté et al. 2009; Teobaldelli et al. 2007). Although this technology would be of great benefit for forest planning and monitoring, tree physiology, and conservation studies, the technology also has limitations. Compared to other sensor technologies, terrestrial laser scanning is restricted by its short and limited working range. Whereas the technology, in principle, allows for the ranging of objects beyond 50 m, the capacity to map trees is much reduced due to occlusion. This phenomenon is especially encountered in the upper canopy, where the ability of terrestrial laser scanning to map distant objects is limited due to occlusion by branches, twigs, and leaves or needles. Other disadvantages are the high costs per area for acquisition and data processing (Wulder et al. 2008). Nevertheless, TLS still holds great promise for future forest research and forest management. TLS is capable of acquiring levels of detail far beyond what airborne and spaceborne laser scanning are capable of. This, by itself, leads to the idea that TLS has potential use for calibrating and evaluating data obtained from airborne and spaceborne LiDAR acquisitions (Zhao and Popescu 2009). An overview of available commercial TLS systems is provided by Fröhlich and Mettenleiter (2004), along with their technical

Table 3 Overview of GLAS-derived height and biomass estimates and their accuracies

Reference	Species/location	Maximum tree height	Canopy height	Timber volume	Results
Lefsky et al. (2005a)	USA, Amazon	✔			$R^2 = 0.59$–0.68; RMSE = 4.85–12.66 m
Lefsky et al. (2007)	USA, Amazon		✔		$R^2 = 0.83$; RMSE = 5 m
Rosette et al. (2008)	Norway spruce, Douglas fir, Scots pine, Corsican pine, Japanese larch, common alder (UK)	✔			$R^2 = 0.9$; RMSE = 2.86 m
Ranson et al. (2007)	Central Siberia			✔	$R^2 = 0.68$; RMSE = 99 $m^3 ha^{-1}$

specifications and the available software for processing the scanner data. Additional information about principles behind the use of range measurements acquired from TLS has been provided by Maas et al. (2008), Bienert et al. (2006), and Aschoff and Spiecker (2004).

Tree detection and stem diameter measurement

Stem diameters are typically derived from ground-based laser scanning data by fitting circles, cylinders or free form curves to the point cloud and these optimization procedures are critical for tree and stem detection. Optimization of the fit is typically achieved through a least squares adjustment or Hough transform (Hough 1962; Tansey et al. 2009). Using least squares adjustment, segmentation of the main stem and any branches into separate classes is important and failing to do so can cause least squares fitting approaches to perform poorly. Hough transform, on the other hand, is less sensitive to outliers but its implementation is computationally more intensive and the technique is primarily for shape detection rather than measurement (Tansey et al. 2009). A variety of studies have pursued the detection and segmentation of branches prior to circle fitting through least squares adjustment, in order to improve diameter estimates.

Hopkinson et al. (2004) applied a cylindrical least squares adjustment to find DBH from TLS points between 1.25 and 1.75 m above the ground. Henning and Radtke (2006) used multi-scan terrestrial LiDAR for the retrieval of stem diameters from loblolly pine (*Pinus taeda* L.) in central Virginia. A detailed description of the processing of the LiDAR point cloud data was provided, both for locating tree centres, and diameter measurements. Since merging of scans resulted in a higher number of surface points, the stem centre-finding algorithm was reapplied after co-registration and this resulted in more accurate stem centre finding. LiDAR-derived diameter measurements overestimated field measurements to some extend but estimates were in close agreement. The average error was <1 cm for measurements below the base of the live crown, and <2 cm for heights up to 13 m. In order to correct for this overestimation, the 10th percentile of the initial diameter estimates was used, resulting in an average error of −0.2 cm and SD = 2.1 cm. The average error increased above 10 m height and peaks in the diameter profiles corresponded to visible whorls on the tree stem. Thies et al. (2004) described and validated an algorithm used for the reconstruction of tree stems, based on cylinder fitting of point clouds obtained from terrestrial laser scanning. The algorithm was tested on a European beech tree (*Fagus silvatica*) and a wild cherry tree (*Prunus avium* L.). The algorithm iteratively searches for cylinders, the parameters of which are orientation and radius that closely fit to the point cloud data representing part of the tree stem. To cover the full extent of the tree stem and to account for taper and stem crookedness, multiple overlapping cylinder segments were used. In addition to the constraint that cylinder segments had to fit the point cloud data to a predefined extent based on a fit statistic, the segments had to fulfil criteria of deviation and orientation relative to previous cylinder segments, corresponding to lower parts of the stem. The algorithm was capable of not only measuring DBH, but also the height of the crown base, taper, sweep, and lean. Since the algorithm was evaluated only in a pilot study, the robustness of the approach needs to be verified in a wide range of tree types. Thies and Spiecker (2004) presented results from the applications of this algorithm on a mixed stand of beech, oak (*Quercus* spp.) and silver-fir (*Abies alba*). Individual tree locating was accurately achieved and was compared to ground reference data. However, the retrieval of most other structural parameters was poor, showing high standard errors in the estimates. The differences in estimates between vertex measurements and laser scans ranged from 54.6 to 190.7% of total length for the variety of tree species included in the study. Differences between DBH measurements determined manually by tape and from laser scans ranged between 82.3 and 109.5% for single scans, and between 84.0 and 111.6% for multiple scan data. Bienert et al. (2006b, 2007) and Maas et al. (2008) presented an algorithm, similar to the one presented by Thies et al. (2004) discussed above, that automatically calculates stem profile, DBH, and stem height. After a pre-processing step in which a DTM is generated, objects are determined by clustering the point cloud using a moving window. Subsequently, circles are fitted through the objects at different heights. If an optimized circle fit is found with small RMSE and the fits comply with the error margins related to the tree class, the segment is classified as stem. DBH is calculated from the DTM using the nearest, most vertical normal vector. When tested on different forest plots, ranging from mixed forest to beech and spruce monocultures, the algorithm showed a few commission and omission errors in the classification of objects as trees (max. omission = 2 vs. max. commission = 3). DBH measurements were conducted accurately with a bias not exceeding 1 cm and a standard deviation around 1.2–2.5 cm. Computation time for the algorithm to process the laser scanner data was on average 5 min but varied with plot type, and took a maximum of 10 min for a 206 MB scan from a mixed forest plot. However, besides the computation time needed to process the scans, considerable time was needed for the forest plot to be referenced with reflective panels before the actual laser acquisition took place. Bienert et al. (2006a) presented results from this algorithm based on RIEGL LMS Z420i scans from a Saxonian mixed forest, where 95% of the

trees could be detected correctly, tree heights could be detected with an accuracy of 80 cm, and DBH could be estimated with a bias less than 1.5 cm. Tansey et al. (2009) compared Hough transform and least squares circle and cylinder fitting to detect tree stems and DBH. Hough transform was deemed a practical technique for stem detection; however, careful selection of parameter ranges was needed. The technique further allows DBH retrieval with reasonable accuracy (SD = 2.3 cm). Nevertheless, due to the lower complexity, higher efficiency, and robustness, the least squares circle adjustment was recommended, although cylinder fits may perform better for leaning stems. Brolly and Király (2009) introduced a least squares adjustment where three circles were fitted at heights, $h = 1$, 1.5 and 2 m above DTM of which at least two needed to match closely. It was found that this approach of comparing independently obtained fit parameters worked better than using a single fitted circle for tree detection but slightly underperformed compared to the cylinder fit for DBH and tree height estimation. Most of these studies have been conducted on trees that show a typical cylindrical stem shape as is often encountered in forest stands of pine and spruce and in forests that are managed for timber production. However, when the intention is to use TLS for rougher stem shapes or in situations that entail a level of detail in the stem cross section for which circles and cylinders no longer provide the ideal geometry, free form curves are needed. Pfeifer and Winterhalder (2004) demonstrated the use of B-splines to represent tree stem cross sections and to account for ovality and occurrence of burls and other irregularities in the tree stem.

Tree height

Tree height has been retrieved from TLS with limited success, compared to airborne LiDAR. Often, tree height is taken as the maximum LiDAR return height within a radial distance from detected tree locations or is based on detected stem taper and taper functions (Király and Brolly 2007). Hopkinson et al. (2004) found that LiDAR data underestimated mean plot-level tree height by 1.5 m compared to the field measurements. Whereas point cloud data were manually processed for the segmentation of individual trees, the researchers argued that automated tree segmentation would be possible for stands with a single canopy layer, little undergrowth, and a low degree of overlapping crowns. Other studies have found similar or larger errors, ranging from RMSE = 1.4–4.4 m (Fleck et al. 2007; Maas et al. 2008; Brolly and Király 2009). Wezyk et al. (2008) compared airborne and terrestrial LiDAR data against field inventory data and found slightly higher estimate errors and underestimate for terrestrial scanning (bias = −0.98 m, SD = 2.18 m) compared to airborne LiDAR (bias = −0.12 m, SD = 1.81 m). A similar finding was made by Tansey et al. (2009) who recommended ALS to estimate tree height rather than TLS as a result of the inherent occlusion effects and increasing point spacing and the related uncertainly as to whether the highest returns are echoes from the tree tops or echoes from inside the tree canopy.

Leaf area

Strahler et al. (2008) and Jupp et al. (2009) used full waveform terrestrial data that are currently exclusively available from the Echidna® scanner to calculate LAI and foliage profiles. First, the gap probability of the canopy is computed based on distance at which the laser pulses are intercepted by the canopy. With decreasing zenith angles, variance of the gap probability increases with potentially large gaps near zenith due to clumping of the canopy and profound segmentation of tree crowns. At increasing zenith angles, this effect is compensated and both vertical and horizontal components of leaf area are accounted; however, with too large a zenith angle, path lengths increase and laser echoes may ultimately become too weak to be detected. Good results have been found near 60° zenith angles (Jupp et al. 2009). Leaf area, L, as a function of height, h, in the canopy is calculated using: $P_{\text{gap}}(\theta, h) = e^{-G(\theta)L(h)/\cos\ \theta}$, where θ is the zenith angle, $G(\theta)$ is the Ross G-function expressing mean projected leaf area in direction θ. Integration over zenith angles gives total leaf area and divided by plot area, one derives LAI. Others have reported the accurate retrieval of LAI and gap fraction from discrete return TLS (Danson et al. 2007; Moorthy et al. 2008). Errors from LAI estimates have been reported to range between 0.2 and 0.3 (Moorthy et al. 2008; Jupp et al. 2009) and are considered accurate in comparison with other techniques currently available (Zhao and Popescu 2009).

Effect of occlusion, tree density, and branching frequency

Effects of stocking density on TLS metrics were reported by Watt and Donoghue (2005) where the capacity of ground-based laser scanning was investigated at different degrees of tree density and branching frequencies. They found that with increasing tree density and increasing branching frequency, the quality of the information obtained from the scanner decreased. For a stand with a density of 600 trees ha^{-1}, laser-derived DBH measurements underestimated reference measurements taken from the field by 4 cm at maximum. Errors in tree count have been reported by a number of studies and reports have been

made up to 0–13% undetected trees (Murphy 2008; Bienert et al. 2006, 2007; Király and Brolly 2007) although up to 37% occlusion has been reported (Murphy 2008). To some extent, the increase of scanning positions can overcome effects of occlusion, although at an increased labour cost. For stocking densities around 1,000 trees ha^{-1} and using four instead of two scanning positions, Tansey et al. (2009) found more accurate basal area estimates and tree counts. Occlusion in medium and dense canopies can also lead to inaccuracies in tree height determination as tree tops and stem locations are difficult to match up in the laser scanned data and attempts have been made to overcome, to some extent, the effects of occlusion through extrapolation of the occluded stem based on lean and curvature of the lower, visible stem (Király and Brolly 2007).

Branch recognition

Bucksch and Lindenbergh (2008) presented the CAMPINO (Collapsing And Merging Procedures In Octree-graphs) algorithm for geometric tree skeleton reconstructions of which centeredness and topology are 'provable good' (Bucksch and Fleck 2009). The algorithm iteratively divides the point cloud space into octree cells. Subdivision of octree cells is terminated based on the cell size and the configuration of points that are within a threshold distance from the cell sides. From the octree subdivision, a graph is constructed by connecting vertices placed on either cell midpoints or cell side midpoints. Simplification of the graph is a final step in which cycles and knots are removed. The skeletonization of the tree structure allows for the measure of branch lengths and diameters for various branch orders. Differences in automatically and manually measured branch lengths are greatest among small branches (higher number of small segments from automatically detected branches) and good results were found in the middle class of branch lengths for seven fruit trees included in the study (Bucksch and Fleck 2009). Gorte and Winterhalder (2004) addressed the issue of recognizing linear structures and retrieving branch topology in point clouds obtained from laser scanning. Their approach was to convert the point cloud into a 3D voxel space and to apply the 8-subiteration method to thin the objects by 'peeling off' the outside layers until a minimum was reached. From these skeletons, graphs were produced with nodes represented by the voxels occupied by the skeleton. The branch topology was determined by using Dijkstra's algorithm: an algorithm to find the shortest routes in graphs, which can be used effectively to resolve the occurrence of loops in the branching structure of the skeletonized tree graph. Other approaches to branch recognition include Hough transform (Fleck et al. 2004) and filtering procedures specifically aimed to remove branching from the LiDAR point clouds as to improve least squares adjustments for circle fitting (Liang et al. 2008).

Tree reconstruction

Recent work has focused on the reconstruction of standing trees, including branches, twigs, and leaves into 3D virtual models that explain effects of the canopy internal structure on CO_2 and water exchange and intra-canopy radiation regimes and to improve our physiological understanding of tree growth (Teobaldelli et al. 2007). Research to date has focused on the reconstruction of individual trees and currently may require intensive manual labour. Fleck et al. (2004) studied the acclimation of leaves to the radiative conditions within tree crowns by reconstructing beech trees from laser scanner data. Segmentation of the point cloud into individual trees was achieved using a Hough transform (Hough 1962) to detect straight line segments in the point cloud. To overcome effects of partial occlusion, line segments were grouped if candidate group members had small angular and spatial displacement. Leaf distribution throughout the tree crowns was measured by constructing polyhedra around the leaf mass of each individual branch contained in the tree crown. The vertices for these polyhedra were obtained from LiDAR returns from a reflector that was positioned by hand. Leaf area was calculated within these polyhedra assuming a constant ratio with branch diameter. The model allowed the calculation of the radiation regime after dividing the crown into height layers and radial sections for which leaf area densities are derived from polyhedral volumes and leaf area, and treating each section as a turbid medium. Whereas Fleck et al. (2004) used aggregates of leaves as turbid media, other reconstruction approaches aim at populating reconstructed crowns with individual leaves. Reconstruction of trees that yield structurally resembling trees typically starts with a reconstruction of tree stem and main branches upon which twigs and leaves are modelled. Xu et al. (2007) initially used single scan data to reconstruct an American Elm tree (*Ulmus Americana*). Reconstruction was achieved using Dijkstra's algorithm to find the shortest path between any point in the LiDAR point cloud and a user selected root point. Path lengths are binned and centroids of the binned points are computed. Branches not included in this main skeleton, as a result of occlusion, are connected based on their alignment and distance with respect to the main skeleton. Remaining points in the point cloud serve as leaf locations to which smaller branches are grown through simulation ensuring that branches are constructed to support as many leaf locations as possible. It was found and shown that single scan data, depending on species, can result in reconstructions with too sparse a leaf area and branching complexity and that this can be overcome through multi-scanning. A similar approach to reconstruction was

chosen by Côté et al. (2009) who acquired terrestrial laser scans made at several (3–5) positions. Tree stem and branches were reconstructed after thresholding intensities to classify returns from wood and leaves. A woody skeleton was obtained using the Dijkstra algorithm and k nearest neighbours to cluster points into components forming the stem and main branches. Branches and leaves that are not included in the scanner data due to occlusion and resolving power of the scanning device were added onto the derived tree skeleton at the locations of likeliness by iteratively calculating light availability and adding branch and foliage components. As a result of limitations in the scanner resolution, the leaf allocation in reconstructed trees may differ from the real trees and future research is needed to yield tree models that more accurately describe foliage distribution throughout the tree crown that can be used in physiological studies.

Hand-held, mobile scanning systems

Besides the industrial laser scanning systems for ground-based forest inventories, a few studies have been published that present the concept of hand-held laser scanning systems that enable fast and cheap acquisition of parameters such as canopy height profile, or the classical inventory parameters that are conventionally measured using clinometers, callipers, tapes, etc., and which are rather time-consuming to obtain compared to those using their laser counterparts. Parker et al. (2004) described the design and creation of a portable LiDAR system for the acquisition of canopy height profiles along linear transects. The system (US$12,000 as of 2003) facilitated the derivation of canopy cover, canopy area index (similar to LAI, but includes woody material), and canopy height, with reasonable accuracies compared to manual approaches. Kalliovirta et al. (2005) developed a laser-relascope for measuring stem diameters and heights. The system uses distance and angle information to determine the diameter and tree height. While the distance is measured using a laser range-finder, an inclinometer is used to measure the angle between the lines tangential to the outer sides of the stem, passing between a variable-width slot, and starting from the standpoint of the observer. A GPS receiver is used to georeference all sample points. Diameter measurements were nearly unbiased (overestimation of 1.3 mm) and showed a standard error of 8.2 mm. Tree height estimates were unbiased with a standard error of 4.9 dm.

Data fusion

The apparent value of LiDAR remote sensing to forest inventories validates the further development and improvement of LiDAR techniques. Tansey et al. (2009) argued that future research focussing on the synergetic use of terrestrial and airborne LiDAR is needed to better explain a bundle of biophysical parameters such as tree height, DBH, stem taper, and volume. Besides the development of techniques that solely rely on LiDAR data, the fusion of LiDAR remote sensing with other types of data acquisition techniques deserves more attention. Several studies have outlined the gain in parameter retrieval that the fusion of different (remote sensing) data could provide and have shown that combining techniques could lower the cost involved in the accurate retrieval of forest structural parameters considerably. For example, Hilker et al. (2008) used Quickbird data to extrapolate LiDAR-derived stand height estimates to more extensive forest areas, for stands of Douglas fir, western red cedar (*Thuja plicata Donn ex* D. Don), western hemlock, and small stands of red alder (*Alnus rubra* Bong.) on Vancouver Island, Canada. This technique was exploited to investigate the potential of increasing the cost effectiveness of remote sensing supported forest inventories. The extrapolation was based on an eCognition (Definiens AG, Germany) classification of the QuickBird data set based on scale, smoothness, shape, colour, and compactness, and it was visually tested whether such derived classes adequately covered the variation in retrieved tree heights from LiDAR data. The extrapolated LiDAR data correlated well with field-based inventories, conducted earlier, and the anticipated tree growth from the date of this field inventory ($R^2 = 0.87$, $P < 0.05$). In Leckie et al. (2003), multispectral data and LiDAR data were combined to increase the performance of delineating tree crowns in Douglas-fir stands of varying densities on the west coast of Canada. Whereas automated delineation of tree crowns achieved an 80–90% overall accuracy compared to ground reference measurements, results showed that the delineation was performed poorly for open plots where the impact of ground vegetation was an apparent problem. This resulted in too many false trees being delineated (commission errors). The problem was greatly reduced using height filters on the delineated tree crowns. The two techniques were found to be complementary to each other, since LiDAR data alone yielded a poor representation of the crowns with fewer commission errors while multispectral data yielded a good representation of the tree crowns but resulted in many commission errors. The data were acquired with a relatively simple Kodak camera (2 × 3 MegaPixel) and a proprietary LiDAR scanning system. The authors emphasized the capacity of LiDAR to retrieve structural parameters better than multispectral remote sensing can, but also its inability to derive species and health attributes. For these attributes, passive optical techniques should be used. McCombs et al. (2003) found opposing results for individual tree

identification, showing that multispectral imagery proved better in delineating individual tree crowns than LiDAR data, but not as good as the fused data set. Average tree height, however, was best determined using LiDAR data only, without multispectral data. Improvements in the retrieval of structural parameters were explained from the reduction in commission errors through fusion with multispectral data. It was pointed out that incorrect registration of geographic coordinates in the multispectral imagery could be reduced through orthorectification, using the LiDAR data as an elevation model. An attempt to fuse LiDAR and hyperspectral data through the application of radiative transfer modelling was successfully achieved by Koetz et al. (2007). They showed that fusion of large footprint LVIS LiDAR and hyperspectral APEX data increased the retrieval accuracy of forest biophysical and biochemical parameters, by using LiDAR height, LAI, and fractional cover estimates to constrain RTM solutions. Hyperspectral data could then be used to select, from this preselected subset of possible RTM inversions, the solution that best corresponded to the found spectral signature. Expected to be of great interest to future forest monitoring studies, of which forest inventory studies are part, is the integration of forest modelling and remote sensing technology (e.g. Schaepman 2007; Smith et al. 2008). Examples of such forest modelling technology are forest growth models such as 3-PG and LPJ-GUESS, and forest fire models such as FARSITE (Andersen et al. 2005; Riaño et al. 2003; Smith et al. 2008). Such approaches could be adopted for the forecasting of NPP, stored carbon, future timber volumes, and the effects of environmental or climatic change on the future forest estate. Ideally, the integration of modelling approaches and remote sensing would include both LiDAR and multi/hyperspectral data to overcome the spectral and spatial limitation of either technique. Not only would remote sensing be useful to support the development of such forest growth and/or fire models, these models also aid in the interpretation of remote sensing data, and they provide a means to identify gross errors and biases in remote sensing data that would otherwise go undetected. That is to say that complementarities between remote sensing data and forest modelling exist that can be exploited to overcome (growing) biases and data inconsistencies.

Comparisons

Practical use of remote sensing as part of inventories of large areas has been demonstrated by several studies described in this paper. The main advantages of spaceborne and airborne LiDAR remote sensing, compared to classical field inventories/measurements, are its fast acquisition time, and the acquisition of tree metrics for large areas (Lovell et al. 2005). The continuous mapping of forest structure allows for the detection of anomalous growth otherwise neglected through plot-based inventories (Donoghue et al. 2007). Airborne LiDAR is currently the most viable option for forest inventories. Its smaller footprint size allows smaller objects to be more accurately resolved in the data than satellite LiDAR. Moreover, data from discrete return, small footprint, high sampling density LiDAR, have been shown to allow for the retrieval of similar information as full waveform LiDARs do (e.g. Morsdorf et al. 2004; Riaño et al. 2003). A considerable disadvantage of satellite-based GLAS LiDAR is non-continuous sampling. Whereas it does nearly cover the Earth from pole to pole, the LiDAR footprints cover the Earth surface just sparsely, greatly limiting the use of the data for forest inventories. Nevertheless, use of additional, continuous data in combination with GLAS footprints has been shown a successful approach for national inventories (Simard et al. 2008), and future spaceborne LiDAR missions are critically important for carbon and biodiversity modelling at the global scale. A clear distinction in forestry applications between airborne and spaceborne LiDAR on the one hand and terrestrial laser scanning on the other has evolved from the very fundamental differences in viewing geometries and resolution. TLS is now used for the reconstruction of trees and stands into virtual 3D models that allow a variety of tree physiological studies to be conducted and is used for pre-harvest assessment of timber volume, stem crookedness, and measurement of diameter profiles. Detailed mapping of the canopy complexity provides a basis for exploring a wide range of crown attributes that are likely to reveal a great deal about site conditions and the prevailing environmental and ecological processes. The high mapping resolution attained with terrestrial laser scanning also indicates potential for the verification and calibration of aerial- and satellite-based remote sensing techniques (Tansey et al. 2009). Finally, in contrast to passive optical techniques, LiDAR has the advantage of having the capacity to directly retrieve structural characteristics, which easily unites this technique with the classical metrics that have been used in forest inventories. For example, Lefsky et al. (2001) compared forest structural parameters obtained from SLICER waveform data with AVIRIS-, Landsat TM-, and ADAR-derived estimates and found that SLICER performed best in the retrieval of basal area, biomass, DBH, maximum height, and number of stems.

Discussion

The potential value of LiDAR remote sensing to future forest monitoring is obvious given the capacity of LiDAR

to produce objective assessments of the 3D forest structure. A long debated problem relating to forest monitoring and inventorying is the subjectivity of such assessments. Even though efforts have been made to define and prescribe indicators of biodiversity to make forest inventories more objective to allow for comparisons of forest stands with regard to their ecological value (Lindenmayer 2000; Noss 1999; Parkes et al. 2003), subjectivity remains a source of uncertainty for many forest managers and planners, especially when the management planning decisions involve large areas, e.g. in planning tasks at national and regional government levels. Since many of these biodiversity indicators are structure related, LiDAR remote sensing holds great promise to fulfil the need for objective, reproducible measurements. Potential use of LiDAR remote sensing has been demonstrated in several of the studies referred to in this paper, in which various structural forest characteristics were derived from LiDAR data. In these studies, the emphasis has been on the derivation of tree height estimates. The use of airborne and spaceborne LiDAR data for the derivation of canopy height profiles is another instance that illustrates the potential of this new technology for use in forestry and for improvements in the capacity of forest workers to collect data to assist forest management and support decision-making. The concept of canopy height profiles, namely that of heights above a forest floor, corresponds to the measurements taken from laser altimetry. Many of the structural forest parameters of interest to forest inventories, such as biomass, DBH and timber volumes, are not directly measured as is the case for height measurements, but inferred using statistical relationships with tree height and crown size. This is not to say that such parameters are less suited for spaceborne and airborne LiDAR remote sensing, but their relationship with LiDAR measurements needs to be understood to better interpret the value of laser altimetry for forest monitoring. Problems related to the use of spaceborne and airborne LiDAR remote sensing are the incorrect sampling of tree tops and the porosity of the tree tops to LiDAR (Gaveau and Hill 2003; Morsdorf et al. 2004). This causes many of the LiDAR-derived height assessments to underestimate the actual tree height. Whereas this phenomenon can be partially corrected for in regression equations, future studies adopting physical modelling approaches—contrary to empirical relationships—are needed to correct for this bias. In addition, as the relative error in tree height estimates increases with decreasing tree height, trees of young age or small stature may not be measured accurately using LiDAR.

Another important field of application of LiDAR technology is the fusion with passive optical remote sensing and can be used to constrain, or validate, structural biophysical parameters used in radiative transfer modelling. Recent studies have investigated the potential of multi-waveband LiDAR to improve modelling of physiological processes in the forest canopy (Morsdorf et al. 2009). Furthermore, spatially continuous passive optical remote sensing is complementary to the non-continuous sampling pattern of LiDAR, and spectral information can aid in the interpretation of point cloud data. Synergies can also be expected from the fusion of these remote sensing technologies for future modelling purposes, such as forest growth modelling and forest fire modelling or to enhance the information extraction of past data acquisitions. St-Onge et al. (2008) used LiDAR to enhance information extraction from passive optical data. They compared the accuracy of CHMs obtained from a combination of photogrammetrically derived DSMs, with CHMs that were produced from LiDAR-derived DSMs (in either case, an accurate LiDAR DTM was used). The results indicated that the CHMs derived through the use of photogrammetry correlated well with their LiDAR counterparts, up to an R^2 of 0.89.

The development and use of fractal indices that explain environmental conditions that drive forest growth is a field of research that needs further investigation over the coming years. Based on the findings of, e.g. Boudon et al. (2006) and Alados et al. (1999) who have explored the dependency of fractal plant geometry on prevailing ecological and management conditions, consideration should be given to the development of fractal indices that can be derived from TLS data. Such fractal indices could either be based on simple box-counting methods, or—more complex—on node lengths against node order. However, besides these fractal indices, a need also exists to develop simpler structural indices—not necessarily based on fractal geometry—that encapsulate the full 3D information content of LiDAR data. Such indices could be designed to quantify the degree of complexity in the plot's canopy, the canopy stratification, and the occurrence of burls, crookedness, and crevices in the tree stems that provide habitat for various insects and animals (Parkes et al. 2003).

In this paper, we have presented an overview of how LiDAR remote sensing can be used today to derive forest structural attributes, and we have addressed approaches for fusing LiDAR data with passive optical techniques. Probably, the greatest advancement to be made in remote sensing would be the fusion of various remote sensing techniques. The profound value of LiDAR in the fusion of remote sensing techniques comes from its very capacity to acquire precise 3D structural information, with greater accuracy than radar techniques allow for. Adding this information to passive optical or radar data enables one to reduce uncertainty in parameter estimates compared to what can be obtained through the use of either of the techniques individually. For this reason, we expect LiDAR

remote sensing—fused with passive optical techniques—to attract growing attention in forest ecosystem, biomass, and biodiversity studies, over the coming years.

Acknowledgments We would like to thank COFORD (the Irish National Council for Forest Research and Development) for funding the FORESTSCAN project, through which this research was made possible, and two anonymous reviewers for their constructive feedback.

References

Alados CL, Escos J, Emlen JM, Freeman DC (1999) Characterization of branch complexity by fractal analyses. Int J Plant Sci 160:s147–s155

Andersen H-E, McGaughey RJ, Reutebuch SE (2005) Estimating forest canopy fuel parameters using LiDAR data. Remote Sens Environ 94:441–449

Anderson JE, Plourde LC, Martin ME, Braswell BH, Smith M-L, Dubayah RO, Hofton MA, Blair JB (2008) Integrating waveform LiDAR with hyperspectral imagery for inventory of a northern temperate forest. Remote Sens Environ 112:1856–1870

Aschoff T, Spiecker H (2004) Algorithms for the automatic detection of trees in laser scanner data. Int Arch Photogramm Remote Sens Spat Inf Sci XXXVI, part 8/W2:71–75

Bienert A, Maas H-G, Scheller S (2006a) Analysis of the information content of terrestrial laserscanner point clouds for the automatic determination of forest inventory parameters. ISPRS WG VIII/11 & EARSeL joint Conference '3D Remote Sensing in Forestry', Vienna, Austria, 14–15 February

Bienert A, Scheller S, Keane E, Mullooly G, Mohan F (2006b) Application of terrestrial laser scanners for the determination of forest inventory parameters. In: Maas H-G, Schneider D (eds) Proceedings of ISPRS commission V symposium 'Image engineering and vision metrology', ISPRS, Dresden, Germany, 25–27 September

Bienert A, Scheller S, Keane E, Mohan F, Nugent C (2007) Tree detection and diameter estimations by analysis of forest terrestrial laser scanner point clouds. ISPRS Workshop on Laser Scanning 2007 and SilviLaser 2007, Espoo, Finland, pp 50–55, 12–14 September 2007

Blair JB, Rabine DL, Hofton MA (1999) The laser vegetation imaging sensor: a medium-altitude, digitisation-only, airborne laser altimeter for mapping vegetation and topography. ISPRS J Photogramm Remote Sens 54:115–122

Boudon F, Godin C, Pradal C, Puech O, Sinoquet H (2006) Estimating the fractal dimension of plants using the two-surface method: an analysis based on 3D digitized tree foliage. Fractals 14:149–163

Brandtberg T, Warner TA, Landenberger RE, McGraw JB (2003) Detection and analysis of individual leaf-off tree crowns in small footprint, high sampling density lidar data from the eastern deciduous forest in North America. Remote Sens Environ 85:290–303

Breidenbach J, Næsset E, Lien V, Gobakken T, Solberg S (2010) Prediction of species specific forest inventory attributes using a nonparametric semi-individual tree crown approach based on fused airborne laser scanning and multispectral data. Remote Sens Environ 114:911–924

Brolly G, Király G (2009) Algorithms for stem mapping by means of terrestrial laser scanning. Acta Silv Lignaria Hung 5:119–130

Bucksch A, Fleck S (2009) Automated detection of branch dimensions in woody skeletons of leafless fruit tree canopies. SilviLaser 2009, Austin, Oct 14–16

Bucksch A, Lindenbergh R (2008) CAMPINO—a skeletonization method for point cloud processing. ISPRS J Photogramm Remote Sens 63:115–127

Chen Q, Baldocchi D, Gong P, Kelly M (2006) Isolating individual trees in a savanna woodland using small footprint lidar data. Photogramm Eng Remote Sens 72:923–932

Coops NC, Hilker T, Wulder M, St-Onge B, Newnham G, Siggins A, Trofymow JA (2007) Estimating canopy structure of Douglas-fir forest stands from discrete-return LiDAR. Trees 21:295–310

Côté J, Widlowski J, Fournier RA, Verstraete MM (2009) The structural and radiative consistency of three-dimensional tree reconstructions from terrestrial lidar. Remote Sens Environ 113:1067–1081

Danson FM, Hetherington D, Morsdorf F, Koetz B, Allgöwer B (2007) Forest canopy gap fraction from terrestrial laser scanning. IEEE Geosci Remote Sens Lett 4:157–160

Donoghue DNM, Watt PJ, Cox NJ, Wilson J (2007) Remote sensing of species mixtures in conifer plantations using LiDAR height and intensity data. Remote Sens Environ 110:509–522

Drake JB, Weishampel JF (2000) Multifractal analysis of canopy height measures in a longleaf pine savanna. For Ecol Manag 128:121–127

Drake JB, Dubayah RO, Clark DB, Knox RG, Blair B, Hofton MA, Chazdon RL, Weishampel JF, Prince SD (2002) Estimation of tropical forest structural characteristics using large-footprint LiDAR. Remote Sens Environ 79:305–319

Flamant PH (2005) Atmospheric and meteorological LiDAR: from pioneers to space applications. Comptes Rendus Phys 6:864–875

Fleck S, Van der Zande D, Schmidt M, Coppin P (2004) Reconstructions of tree structures from laser-scans and their use to predict physiological properties and processes in canopies. Int Arch Photogramm Remote Sens Spat Inf Sci XXXVI part 8/W2:118–123

Fleck S, Obertreiber N, Schmidt I, Brauns M, Jungkunst HF, Leuschner C (2007) Terrestrial LiDAR measurements for analysing canopy structure in an old-growth forest. Int Arch Photogramm Remote Sens Spat Inf Sci XXXVI part 3/W52:125–129

Fröhlich Z, Mettenleiter M (2004) Terrestrial laser scanning—new perspectives in 3D surveying. Int Arch Photogramm Remote Sens Spat Inf Sci XXXVI part 8/W2:7–13

Gaveau DLA, Hill RA (2003) Quantifying canopy height underestimation by laser pulse penetration in small-footprint airborne laser scanning data. Can J Remote Sens 29:650–657

Gitelson AA (2004) Wide dynamic range vegetation index for remote quantification of biophysical characteristics of vegetation. J Plant Physiol 161:165–173

Goodwin NR, Coops NC, Culvenor DS (2006) Assessment of forest structure with airborne LiDAR and the effects of platform altitude. Remote Sens Environ 103:140–152

Gorte B, Winterhalder D (2004) Reconstruction of laser-scanned trees using filter operations in the 3D raster domain. Int Arch Photogramm, Remote Sens Spat Inf Sci XXXVI part 8/W2:39–44

Gougeon FA (2005) The individual tree crown (ITC) suite. Canadian Forest Service, Victoria

Green AA, Berman P, Switzer P, Craig MD (1988) A transform for ordering multispectral data in terms of image quality with implications for noise removal. IEEE Trans Geosci Remote Sens 26:65–74

Harding DJ, Carabajal CC (2005) ICESat waveform measurements of within-footprint topographic relief and vegetation vertical structure. Geophys Res Lett 32:L21s10

Henning JG, Radtke PJ (2006) Detailed stem measurements of standing trees from ground-based scanning LiDAR. For Sci 52:67–80

Heurich M (2008) Automatic recognition and measurement of single trees based on data from airborne laser scanning over the richly structured natural forests of the Bavarian Forest National Park. For Ecol Manag 255:2416–2433

Hilker T, Wulder MA, Coops NC (2008) Update of forest inventory data with LiDAR and high spatial resolution satellite imagery. Can J Remote Sens 34:5–12

Holmgren J, Persson Å (2004) Identifying species of individual trees using airborne laser scanner. Remote Sens Environ 90:415–423

Holmgren J, Nilsson M, Olsson H (2003) Estimation of tree height and stem volume on plots using airborne laser scanning. For Sci 49:419–428

Hopkinson C, Chasmer L, Young-Pow C, Treitz P (2004) Assessing forest metrics with a ground-based scanning LiDAR. Can J Remote Sens 34:573–583

Hough PVC (1962) Method and means for recognizing complex patterns. US Patent 3,069,654

Hug C, Ullrich A, Grimm A (2004) Litemapper-5600—a waveform-digitizing LiDAR terrain and vegetation mapping system. Int Arch Photogramm Remote Sens Spat Inf Sci XXXVI part 8/W2: 24–29

Jupp DLB, Culvenor DS, Lovell JL, Newnham GJ, Strahler AH, Woodcock CE (2009) Estimating forest LAI profiles and structural parameters using a ground-based laser called 'Echidna®'. Tree Physiol 29:171–181

Kalliovirta J, Laasasenaho J, Kangas A (2005) Evaluation of the laser-relascope. For Ecol Manag 204:181–194

Kato A, Moskal LM, Schiess P, Swanson ME, Calhoun D, Stuetzle W (2009) Capturing tree crown formation through implicit surface reconstruction using airborne lidar data. Remote Sens Environ 113:1148–1162

Király G, Brolly G (2007) Tree height estimation methods for terrestrial laser scanning in a forest reserve. Int Arch Photogramm Remote Sens Spat Inf Sci XXXVI part 3/W52:211–215

Kirchhof M, Jutzi B, Stilla U (2008) Iterative processing of laser scanning data by full waveform analysis. ISPRS J Photogramm Remote Sens 63:99–114

Koetz B, Sun G, Morsdorf F, Ranson KJ, Kneubühler M, Itten K, Allgöwer B (2007) Fusion of imaging spectrometer and LiDAR data over combined radiative transfer models for forest canopy characterization. Remote Sens Environ 106:449–459

Kumar L, Schmidt K, Dury S, Skidmore A (2002) Imaging spectrometry and vegetation science. In: Van der Meer FD, De Jong SM (eds) Imaging spectrometry. Springer, Netherlands, pp 111–156

Leckie D, Gougeon F, Hill D, Quinn R, Armstrong L, Shreenan R (2003) Combined high-density LiDAR and multispectral imagery for individual tree crown analysis. Can J Remote Sens 29:633–649

Lee AC, Lucas RM (2007) A LiDAR-derived canopy density model for tree stem and crown mapping in Australian forests. Remote Sens Environ 111:493–518

Lefsky M, Harding DJ, Cohen WB, Parker GG, Shugart HH (1999) Surface LiDAR remote sensing of basal area and biomass in deciduous forests of eastern maryland, USA. Remote Sens Environ 67:83–98

Lefsky MA, Cohen WB, Spies TA (2001) An evaluation of alternate remote sensing products for forest inventory, monitoring, and mapping of Douglas-fir forest in Western Oregon. Can J Remote Sens 31:78–87

Lefsky MA, Harding DJ, Keller M, Cohen WB, Carabajal CC, Espirito-Santo FDB, Hunter MO, de Oliveira JR (2005a) Estimates of forest canopy height and aboveground biomass using ICESat. Geophys Res Lett 32:L22S02

Lefsky MA, Hudak AT, Cohen WB, Acker SA (2005b) Geographic variability in LiDAR predictions of forest stand structure in the Pacific Northwest. Remote Sens Environ 95:532–548

Lefsky M, Keller M, Pang Y, de Camargo PB, Hunter MO (2007) Revised method for forest canopy height estimation from geoscience laser altimeter system waveforms. J Appl Remote Sens 1:013537

Liang X, Litkey P, Hyyppä J, Kukko A, Kaartinen H, Holopainen M (2008) Plot-level trunk detection and reconstruction using one-scan-mode terrestrial laser scanning data. 2008 International workshop on earth observation and remote sensing applications, IEEE, Beijing, 30 June–2 July

Lillesand TM, Kiefer RW, Chipman JW (2004) Remote sensing and image interpretation. Wiley, Hoboken, NJ

Lim K, Treitz P, Wulder M, St-Onge B, Flood M (2003) LiDAR remote sensing of forest structure. Prog Phys Geogr 27: 88–106

Lindenmayer DB (2000) Indicators of biodiversity for ecologically sustainable forest management. Conserv Biol 14:941–950

Lovell JL, Jupp DLB, Newnham GJ, Coops NC, Culvenor DS (2005) Simulation study for finding optimal LiDAR acquisition parameters for forest height retrieval. For Ecol Manag 214:398–412

Maas H-G, Bienert A, Scheller S, Keane E (2008) Automatic forest inventory parameter determination from terrestrial laser scanner data. Int J Remote Sens 29:1579–1593

MacArthur RH, Horn HS (1969) Foliage profile by vertical measurements. Ecol 50:802–804

Maltamo M, Eerikäinen K, Pitkänen J, Hyppä J, Vehmas M (2004) Estimation of timber volume and stem density based on scanning laser altimetry and expected tree size distribution functions. Remote Sens Environ 90:319–330

McCombs JW, Roberts SD, Evans DL (2003) Influence of fusing LiDAR and multispectral imagery on remotely sensed estimates of stand density and mean tree height in a managed loblolly pine plantation. For Sci 49:457–466

Middleton WEK, Spilhaus AF (1953) Meteorological instruments. University of Toronto Press, Toronto

Moorthy I, Miller JR, Hu B, Chen J, Li Q (2008) Retrieving crown leaf area index from an individual tree using ground-based lidar data. Can J Remote Sens 34:320–332

Morsdorf F, Meier E, Koetz B, Itten KI, Dobbertin M, Allgöwer B (2004) LIDAR-based geometric reconstruction of boreal type forest stands at single tree level for forest and wildland fire management. Remote Sens Environ 92:353–362

Morsdorf F, Koetz B, Meier E, Itten KI, Allgöwer B (2006) Estimation of LAI and fractional cover from small footprint airborne laser scanning data based on gap fraction. Remote Sens Environ 104:50–61

Morsdorf F, Frey O, Meier E, Itten KI, Allgöwer B (2008) Assessment of the influence of flying altitude and scan angle on biophysical vegetation products derived from airborne laser scanning. Int J Remote Sens 29:1387–1406

Morsdorf F, Nichol C, Malthus T, Woodhouse IH (2009) Assessing forest structural and physiological information content of multi-spectral LiDAR waveforms by radiative transfer modelling. Remote Sens Environ 113:2152–2163

Murphy G (2008) Determining stand value and log product yields using terrestrial lidar and optimal bucking: a case study. J For 106:317–324

Myneni R, Nemani R, Running S (1997) Estimation of global leaf area index and absorbed par using radiative transfer models. IEEE Trans Geosci Remote Sens 35:1380–1393

Næsset E (2009a) Effects of different sensors, flying altitudes, and pulse repetition frequencies on forest canopy metrics and biophysical stand properties derived from small-footprint airborne laser data. Remote Sens Environ 113:148–159

Næsset E (2009b) Influence of terrain model smoothing and flight and sensor configurations on detection of small pioneer trees in the boreal-alpine transition zone utilizing height metrics derived

from airborne scanning lasers. Remote Sens Environ 113:2210–2223
Næsset E, Gobakken T (2008) Estimation of above- and below-ground biomass across regions of the boreal forest zone using airborne laser. Remote Sens Environ 112:3079–3090
Næsset E, Økland T (2002) Estimating tree height and tree crown properties using airborne scanning laser in a boreal nature reserve. Remote Sens Environ 79:105–115
Næsset E, Bollandsås OM, Gobakken T (2005) Comparing regression methods in estimation of biophysical properties of forest stands from two different inventories using laser scanner data. Remote Sens Environ 94:541–553
Nelson RF (2008) Model effects on GLAS-based regional estimates of forest biomass and carbon. SilviLaser 2008, 17–19 September, Edinburgh, pp 207–215
Nelson R, Jimenez J, Schnell CE, Hartshorn GS, Gregoire TG, Oderwald R (2000) Canopy height models and airborne lasers to estimate forest biomass: two problems. Int J Remote Sens 21:2153–2162
Noss RF (1999) Assessing and monitoring forest biodiversity: a suggested framework and indicators. For Ecol Manag 115:135–146
Ørka HO, Næsset E, Bollandsås OM (2009) Classifying species of individual trees by intensity and structure features derived from airborne laser scanner data. Remote Sens Environ 113:1163–1174
Parker GG, Harding DJ, Berger ML (2004) A portable LiDAR system for rapid determination of forest canopy structure. J Appl Ecol 41:755–767
Parkes D, Newell G, Cheal D (2003) Assessing the quality of native vegetation: the 'habitat hectares' approach. Ecol Manag Restor 4(supplement):s29–s38
Pfeifer N, Briese C (2007) Geometrical aspects of airborne and terrestrial laser scanning. Int Arch Photogramm Remote Sens Spat Inf Sci XXXVI part 3/W52: 311–319
Pfeifer N, Winterhalder D (2004) Modelling of tree cross sections from terrestrial laser scanning data with free-form curves. Int Arch Photogramm Remote Sens Spat Inf Sci XXXVI part 8/W2: 76–81
Popescu S, Wynne RH (2004) Seeing the trees in the forest: using lidar and multispectral data fusion with local filtering and variable window size for estimating tree height. Photogramm Eng Remote Sens 70:589–604
Popescu SC, Wynne RH, Nelson RF (2002) Estimating plot-level tree heights with LiDAR: local filtering with a canopy-height based variable window size. Comput Electron Agric 37:71–95
Popescu SC, Wynne RH, Nelson RF (2003) Measuring individual tree crown diameter with LiDAR and assessing its influence on estimating forest volume and biomass. Can J Remote Sens 29:564–577
Rahman MZA, Gorte BGH (2009) Tree crown delineation from high resolution airborne lidar based on densities of high points. Int Arch Photogramm Remote Sens Spat Inf Sci XXXVIII part 3/W8:123–128
Ranson KJ, Sun G, Kovacs K, Kharuk VI (2004a) Landcover attributes from ICESat GLAS data in central Siberia. In: Proceedings of international geoscience and remote sensing symposium 2004, 20–24 September. IEEE International, Anchorage, pp 753–756
Ranson KJ, Sun G, Kovacs K, Kharuk VI (2004b) Use of ICESat GLAS data for forest disturbance studies in central Siberia. In: Proceedings of international geoscience and remote sensing symposium 2004, 20–24 September. IEEE International, Anchorage, pp 1936–1939
Ranson KJ, Kimes D, Sun G, Nelson R, Kharuk V, Montesano P (2007) Using MODIS and GLAS data to develop timber volume estimates in central Siberia. In: International Conference on Geoscience and Remote Sensing Symposium 2007, 23–28 July. IEEE, Barcelona, pp 2306–2309
Reese H, Nilsson M, Sandström P, Olsson H (2002) Applications using estimates of forest parameters derived from satellite and forest inventory data. Comput Electron Agric 37:37–55
Reitberger J, Krzystek P, Stilla U (2008) Analysis of full waveform LIDAR data for the classification of deciduous and coniferous trees. Int J Remote Sens 29:1407–1431
Reitberger J, Schnörr C, Krzystek P, Stilla U (2009) 3D segmentation of single trees exploiting full waveform LIDAR data. ISPRS J Photogramm Remote Sens 64:561–574
Riaño D, Meier E, Allgoewer B, Chuvieco E, Ustin SL (2003) Modeling airborne laser scanning data for the spatial generation of critical forest parameters in fire behavior modeling. Remote Sens Environ 86:177–186
Ritchie JC (1996) Remote sensing applications to hydrology: airborne laser altimeters. Hydrol Sci J 41:625–636
Roberts G (1998) Simulating the vegetation canopy LiDAR: an investigation of the waveform information content. Masters, University College London, London
Roberts JW, Tesfamichael S, Gebreslasie M, Van Aardt J, Ahmed FB (2007) Forest structural assessment using remote sensing technologies: an overview of the current state of the art. South Hemisph For J 69:183–203
Rosette JAB, North PRJ, Suárez JC (2008) Vegetation height estimates for a mixed temperate forest using satellite laser altimetry. Int J Remote Sens 29:1475–1493
Sasaki T, Imanishi J, Ioki K, Morimoto Y, Kitada K (2008) Estimation of leaf area index and canopy openness in broad-leaved forest using an airborne laser scanner in comparison with high-resolution near-infrared digital photography. Landsc Ecol Eng 4:47–55
Schaepman ME (2007) Spectrodirectional remote sensing: from pixels to processes. Int J Appl Earth Obs Geoinf 9:204–223
Shi J, Malik J (2000) Normalized cuts and image segmentation. IEEE Trans Pattern Anal Mach Intell 22:888–905
Simard M, Rivera-Monroy VH, Mancera-Pineda JE, Castaneda-Moya E, Twilley RR (2008) A systematic method for 3D mapping of mangrove forests based on shuttle radar topography mission elevation data, ICEsat/GLAS waveforms and field data: application to Ciénaga Grande de Santa Marta, Colombia. Remote Sens Environ 112:2131–2144
Smith B, Knorr W, Widlowski J-L, Pinty B, Gobron N (2008) Combining remote sensing data with process modelling to monitor boreal conifer forest carbon balances. For Ecol Manag 255:3985–3994
St-Onge B, Vega C, Fournier RA, Hu Y (2008) Mapping canopy height using a combination of digital stereo-photogrammetry and LiDAR. Int J Remote Sens 29:3343–3364
Strahler AH, Jupp DLB, Woodcock CE, Schaaf CB, Yao T, Zhao F, Yang X, Lovell J, Culvenor D, Newnham G, Ni-Miester W, Boykin-Morris W (2008) Retrieval of forest structural parameters using a ground-based lidar instrument 'Echidna®'. Can J Remote Sens 34:S426–S440
Sun G, Ranson KJ, Kimes DS, Blair JB, Kovacs K (2008) Forest vertical structure from GLAS: an evaluation using LVIS and SRTM data. Remote Sens Environ 112:107–117
Takahashi T, Kazukiyo Y, Senda Y, Tsuzuku M (2005) Estimating individual tree heights of sugi (*Cryptomeria japonica* D. Don) plantations in mountainous areas using small-footprint airborne LiDAR. J For Res 10:135–142
Tansey K, Selmes N, Anstee A, Tate NJ, Denniss A (2009) Estimating tree and stand variables in a Corsican Pine woodland from terrestrial laser scanner data. Int J Remote Sens 30:5195–5209

Teobaldelli M, Zenone T, Puig D, Matteucci M, Seufert G, Sequeira V (2007) Structural tree modelling of aboveground and belowground poplar tree using direct and indirect measurements: terrestrial laser scanning, WGROGRA, AMAPmod and JRC-3D Reconstructor®. Functional Structural Plant Models, Napier, New Zealand, November 4–9

Thies M, Spiecker H (2004) Evaluation and future prospects of terrestrial laser scanning for standardized forest inventories. Int Arch Photogramm Remote Sens Spat Inf Sci XXXVI part 8/W2:192–197

Thies M, Pfeifer N, Winterhalder D, Gorte BGH (2004) Three-dimensional reconstruction of stems for assessment of taper, sweep, and lean based on laser scanning of standing trees. Scand J For Res 19:571–581

Turner W, Spector S, Gardiner N, Fladeland M, Sterling E, Steininger M (2003) Remote sensing for biodiversity science and conservation. Trends Ecol Evol 18:306–314

Van Leeuwen M, Coops NC, Wulder MA (2010) Canopy surface reconstruction from a LiDAR point cloud using hough transform. Remote Sens Lett 1:125–132

Wagner W, Ullrich A, Ducic V, Melzer T, Studnicka N (2006) Gaussian decomposition and calibration of a novel small-footprint full-waveform digitising airborne laser scanner. ISPRS J Photogramm Remote Sens 60:100–112

Wagner W, Hollaus M, Briese C, Ducic V (2008) 3D vegetation mapping using small-footprint full-waveform airborne laser scanners. Int J Remote Sens 29:1433–1452

Watt PJ, Donoghue DNM (2005) Measuring forest structure with terrestrial laser scanning. Int J Remote Sens 26:1437–1446

Wehr A, Lohr U (1999) Airborne laser scanning—an introduction and overview. ISPRS J Photogramm Remote Sens 54:68–82

Weinacker H, Koch B, Heyder U, Weinacker R (2004) Development of filtering, segmentation and modelling modules for LIDAR and multispectral data as a fundament of an automatic forest inventory system. Int Arch Photogramm Remote Sens Spat Inf Sci XXXVI part 8/W2:50–55

Wezyk P, Tompalski P, Szostak M, Glista M, Pierzchalski M (2008) Describing the selected canopy layer parameters of the Scots pine stands using ALS data. SilviLaser 2008, Edinburgh, Sept 17–19

Wulder MA, Bater CW, Coops NC, Hilker T, White JC (2008) The role of LiDAR in sustainable forest management. For Chron 84:807–826

Xu H, Gossett N, Chen B (2007) Knowledge and heuristic-based modeling of laser-scanned trees. ACM Trans Graph 26:19:1–19:13

Yong G, Zengyuan L, Sun G, Lefsky M, Xinfang Y (2006) Model based terrain effect analyses on ICEsat GLAS waveforms. In: Proceedings of IEEE international conference on geoscience remote sensing symposium 2006, 31 July–4 Aug. IEEE, Denver, pp 3232–3235

Yu X, Hyppä J, Hyppä H, Maltamo M (2004) Effects of flight altitude on tree height estimation using airborne laser-scanning. Int Arch Photogramm Remote Sens Spat Inf Sci XXXVI part 8/W2:96–101

Yu X, Hyyppä J, Kaartinen H, Maltamo M, Hyyppä H (2008) Obtaining plotwise mean height and volume growth in boreal forests using multi-temporal laser surveys and various change detection techniques. Int J Remote Sens 29:1367–1386

Zhao K, Popescu S (2009) Lidar-based mapping of leaf area index and its use for validating GLOBCARBON satellite LAI product in a temperate forest of the southern USA. Remote Sens Environ 113:1628–1645

Zhao K, Popescu S, Nelson R (2009) LiDAR remote sensing of forest biomass: a scale invariant estimation approach using airborne lasers. Remote Sens Environ 113:182–196

Zimble DA, Evans DL, Carlson GC, Parker RC, Grado SC, Gerard PD (2003) Characterizing vertical forest structure using small-footprint airborne LiDAR. Remote Sens Environ 87:171–182